Neurosymbolic Artificial Intelligence
XX(X):2–??

DOI: 10.1177/ToBeAssigned
www.sagepub.com/
SAGE

Propositional Theory Revision through Neural Concept Invention

Sieben Bocklandt[1,2], Vincent Derkinderen[1,2], Wannes Meert[1,2] and Luc De Raedt[1,2,3]

Abstract

Neurosymbolic methods that follow the probabilistic-logic paradigm, such as DeepProbLog or Scallop, combine symbolic background knowledge with neural networks to enable both reasoning and perception. Unfortunately, these models typically assume the knowledge to be perfect and complete. This limits their usability, as it is unrealistic in real-world environments, particularly in domains that require both structured reasoning and perception. To address this issue, we propose a novel methodology that iteratively revises an initial imperfect and incomplete logical background theory with neural concepts. Our approach, termed NeTheR, iteratively revises the symbolic theory through a sequence of greedily selected modifications until no further improvement is expected. Historically, theory revision in inductive logic programming has been achieved by adding or removing symbolic literals to improve logical models. NeTheR extends this by leveraging predicate invention in a propositional setting to introduce neural concept representations. These modifications, such as inserting a neural concept into a specific part of the model, are identified using a variant of the Sharpe ratio that estimates their risk-adjusted performance gain. Empirical evaluation demonstrates that NeTheR effectively revises imperfect probabilistic-logic-based neurosymbolic models across a diverse collection of theory revision tasks, while generally outperforming competing approaches.

Keywords

Theory revision, Neurosymbolic AI, Neural ILP, Probabilistic Logic

1 Introduction

Neurosymbolic AI (NeSy) is an emerging subfield within artificial intelligence (Gartner 2025) that combines the strengths of two traditionally distinct approaches: symbolic reasoning and neural computations. Symbolic AI, which emphasizes logic, rules, and human-like reasoning, excels in handling abstract, structured knowledge and can be easily interpreted by humans (De Raedt 2008; Russell and Norvig 2020). Neural approaches, on the other hand, have contributed significant advances in pattern recognition, perception, and data-driven learning, especially with unstructured data such as images and text. Such neural approaches do, however, often lack explainability, logical consistency, and the ability to generalize from limited data (Rudin et al. 2021). NeSy aims to bridge these gaps, creating systems that cannot only learn from vast amounts of data, but also reason at the same time in a structured, interpretable manner. By integrating neural networks' learning capabilities with symbolic reasoning, many neurosymbolic systems preserve an explicit logical structure while exploiting subsymbolic data. Depending on the degree of neural integration, this comes with different trade-offs between expressiveness and interpretability.

Among the many neurosymbolic paradigms, probabilistic logic programming frameworks such as DeepProbLog (Manhaeve et al. 2021) and Scallop (Li et al. 2023) provide a particularly principled integration of symbolic reasoning and neural perception through arithmetic circuits. Despite recent progress, revising imperfect symbolic knowledge in these systems remains challenging. These systems typically assume that the symbolic program is fixed, while neural components correspond to predefined concepts. When the available symbolic knowledge is incomplete or partially incorrect, automatically refining the symbolic structure remains largely unexplored. In many practical settings, domain experts can provide an initial set of logical rules or background knowledge, but these rules rarely capture the full complexity of the environment (Mooney and Shavlik 2021). While several neurosymbolic approaches can learn symbolic structures jointly with neural representations (Towell and Shavlik 1994; Sourek et al. 2015; Shindo et al. 2021), they often treat the provided knowledge as fixed or rely primarily on learning new structure from data. However, discarding existing knowledge and relearning everything from scratch is undesirable, particularly in low-data regimes where prior knowledge can provide valuable inductive bias (Russell and Norvig 2020; De Raedt 2008). Instead, it is often more natural to start from the

[1]Department of Computer Science, KU Leuven, Belgium
[2]Leuven.AI - KU Leuven Institute for AI, Belgium
[3]Center for Applied Autonomous Systems, Örebro University, Sweden

Corresponding author:
Sieben Bocklandt
Email: sieben.bocklandt@kuleuven.be

available knowledge and refine it where necessary. This perspective aligns with theory revision in logic programming, where imperfect rule sets are incrementally corrected and extended (Mooney and Shavlik 2021). Bringing this principle to neurosymbolic systems allows models to remain faithful to prior knowledge while adapting it based on data.

We address these shortcomings by proposing NeTheR* (**Ne**urosymbolic **The**ory **R**evision), a propositional theory revision framework for probabilistic-logic-based neurosymbolic models. NeTheR incrementally revises an existing symbolic theory by inserting symbolic literals and learned neural concepts. Unlike many existing probabilistic logic programming systems, which assume neural predicates to correspond to predefined concepts (e.g., object or attribute detectors), NeTheR can invent neural concepts whose meaning is not specified beforehand. These neural concepts are learned directly from subsymbolic data and integrated into the symbolic theory where they provide the greatest benefit. This approach combines the advances in neurosymbolic research with the principles of theory revision (Mooney and Shavlik 2021), a field that focuses on refining knowledge bases such as logical rules (Muggleton and Buntine 1988; De Raedt 1992; Ourston and Mooney 1990), or probabilistic networks (Mahoney and Mooney 1993; Ramachandran and Mooney 1996). NeTheR can refine the existing symbolic structure with new, learned concept representations, thus compensating for incomplete knowledge.

Example 1.1. *As an example task, consider a binary classification problem over a collection of photographs. The goal is to classify whether a given picture belongs to the positive class, defined as images that were taken by either Alice or Bob and that depict either a bird or a fish. Additionally, animals photographed by Alice should not have the ability to fly. All other images belong to the negative class. The only annotated information is the available set of Boolean encoded categorical variables:* `Photographer`*,* `Bones`*, and* `Gills`*, abbreviated as P, B, and G respectively. An expert attempts to solve this task using the logic formula below, which is based on expert knowledge that birds have hollow bones and all fish have gills.*

$$(P = Alice \vee P = Bob) \wedge (B = Hollow \vee G = True)$$

This solution is imperfect as it does not cover birds without hollow bones, such as penguins, nor the extra constraint for Alice. Existing symbolic theory revision methods can only revise the symbolic variables already present in the knowledge base. They cannot introduce concepts derived directly from subsymbolic inputs such as images without prior feature extraction. In contrast, NeTheR introduces neural concepts, propositional neural predicates, whose value depends on subsymbolic data, thereby increasing the expressive power of the theory. An example of the result of NeTheR is shown in Figure 1, which includes the introduction of a neural concept and a new symbolic literal to refine the formula. For example, given enough data, the neural concept learns to recognize whether an animal has wings, thus is probably a bird.

*All code will be made publicly available upon paper acceptance.

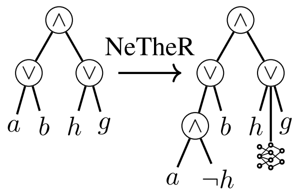

Figure 1. Example initial theory and its revision by NeTheR. We use propositional symbols to describe properties of each image: a denotes that the picture was taken by Alice ($P =$ Alice), b denotes that the picture was taken by Bob ($P =$ Bob), h denotes that the depicted animal has hollow bones ($B =$ Hollow), and g denotes that the depicted animal has gills ($G =$ True). NeTheR introduces a new symbolic literal $\neg h$ to exclude many of the flying animals, and additionally incorporates a neural concept to revise the initial theory.

Our key contribution is the introduction of NeTheR, a framework that (1) improves probabilistic-logic-based neurosymbolic models by refining imperfect background knowledge in a data-driven manner, and (2) extends theory revision with neural concept invention, allowing the system to introduce neural concepts that do not have a predefined semantic interpretation. This enables the model to discover useful intermediate concepts directly from subsymbolic data and incorporate them into symbolic rules. To efficiently identify impactful modifications to the theory, we further propose a variant of the Sharpe ratio that prioritizes revisions with high expected performance gains relative to their uncertainty.

2 Background

We first introduce propositional logic as a foundation for formal reasoning, arithmetic circuits for efficient exact inference on propositional logic, and neurosymbolic AI, which integrates symbolic reasoning with neural networks.

2.1 Propositional Logic

We consider a symbolic input space $\mathcal{X}_S$ consisting of a finite set of feature variables $\mathcal{X}_S = \{X_1, X_2, \dots, X_n\}$, where each feature variable X_i is associated with its own domain $\mathcal{D}_i$. A feature variable may be either categorical, with a finite domain of discrete values, or continuous, with a domain that is a subset of $\mathbb{R}$. An interpretation $I_{\mathcal{X}_S}$ assigns to each feature variable $X_i \in \mathcal{X}_S$ a value $I(X_i) \in \mathcal{D}_i$. To reason about feature variables in propositional logic, we introduce Boolean variables defined by predicates over feature variables, which we call *symbolic literals* in the remainder of this work. A symbolic literal is a Boolean expression of the form $(X_i \bowtie v)$, where $X_i \in \mathcal{X}_S$, $\bowtie$ an (in)equality operator and $v \in \mathcal{D}_i$; each symbolic literal evaluates to true or false under an interpretation I depending on whether the predicate holds for the assigned value $I(X_i)$. A propositional logic formula F is inductively defined as a symbolic literal, a disjunction $F_1 \vee F_2$, a conjunction $F_1 \wedge F_2$, or a negation $\neg F_1$, with the usual Boolean semantics, and therefore acts as a Boolean classifier over the input space $\mathcal{X}_S$, evaluating to true or false for any interpretation $I_{\mathcal{X}_S}$. An interpretation I is said to *satisfy* a formula F, denoted $I \models F$, if F evaluates to true under I. For example, the interpretation $I = \{Colour \mapsto Red,\ Height \mapsto 175\}$ satisfies the symbolic literals $(Colour = Red)$ and $(Height < 180)$, and consequently satisfies the formula $(Colour = Red) \wedge (Height < 180)$.

A *logic circuit* represents a logic formula as a directed acyclic graph of leaf nodes (literals) and inner nodes with an associated type (either disjunction, conjunction, or negation), as shown in Figure 1. Logic circuits explicitly support the reuse of subcircuits, i.e., a node can have more than one parent node. We use the terms logic circuit and logic formula interchangeably throughout this work.

2.2 Tractable Probabilistic Inference in Logic Circuits

While propositional logic provides a deterministic classification mechanism, many real-world applications require reasoning under uncertainty, which can be incorporated by compiling the logic circuit into an equivalent circuit with specific structural properties. These properties allow the compiled circuit to be evaluated under probabilistic semantics, yielding a probabilistic (arithmetic) circuit, and crucially enable tractable probabilistic inference by guaranteeing that circuit evaluation is linear in the size of the circuit. Specifically, a formula must satisfy three structural properties (Darwiche and Marquis 2002): it is in *negation normal form* (NNF) if negation occurs only directly on Boolean variables; it is *decomposable* if, for every conjunction node, the conjunct branches do not share variables; and it is *deterministic* if, for every disjunction node, the disjunct branches are mutually exclusive, meaning that no interpretation satisfies more than one branch simultaneously.

Knowledge compilation algorithms transform an arbitrary logic formula into an equivalent logic circuit satisfying these properties, commonly referred to as decomposable deterministic negation normal form (d-DNNF). These properties guarantee that the resulting circuit admits tractable probabilistic inference. In particular, a d-DNNF circuit can be systematically converted into an arithmetic circuit, enabling efficient computation of probabilities. We use the PySDD (Meert 2017) software package to perform this compilation.

2.3 Arithmetic Circuits

To perform probabilistic inference, each literal l in the compiled circuit is associated with a *probability function* $p_l(\mathbf{x}) \in [0, 1]$, representing the probability that the literal is true given input $\mathbf{x}$. For symbolic literals, this reduces to a Boolean evaluation on symbolic input $I_{\mathcal{X}_S}$:

$$p_l(I_{\mathcal{X}_S}) = \begin{cases} 1 & \text{if } I_{\mathcal{X}_S} \models l \\ 0 & \text{otherwise} \end{cases} \tag{1}$$

Given these probability functions, the compiled logic circuit can be evaluated as an *arithmetic circuit (AC)*. This replaces logical operators with arithmetic operators: conjunction nodes become multiplication, and disjunction nodes become addition, while literal nodes evaluate to their probability functions.

Formally, the arithmetic circuit rooted at node n evaluates as:

$$p_n(\mathbf{x}) = \begin{cases} p_l(\mathbf{x}) & \text{if } n \text{ is a literal } l \\ \prod_{d \in in(n)} p_d(\mathbf{x}) & \text{if } n \text{ is a conjunction} \\ \sum_{d \in in(n)} p_d(\mathbf{x}) & \text{if } n \text{ is a disjunction} \end{cases} \tag{2}$$

with $in(n)$ the input nodes of node n. This arithmetic circuit computes the probability that the logical formula is satisfied given the literal probabilities, and enables exact probabilistic inference in time linear in the circuit size.

2.4 Neurosymbolic AI

In a probabilistic logic circuit, each literal l is evaluated using its associated probability function $p_l(\mathbf{x})$. In a pure inference setting, these probability values are fixed and specified a priori. In a learning setting, however, the probability functions can instead be treated as learnable parameters that are optimized from data. In this case, the circuit defines a differentiable computational structure through which gradients can propagate, allowing the parameters governing the literal probabilities to be learned.

Extending this idea, Manhaeve et al. (2021) proposed parametrizing some literals with the output of a neural network. In their framework, the neural network represents the probability function of the literal. These neural literals, referred to as *neural predicates* in the logic programming setting, allow the system to infer symbolic properties from subsymbolic inputs such as images, while integrating seamlessly into the arithmetic circuit.

In this work, we adopt a similar mechanism, and use the term *neural concepts* to refer to literals nc whose probability function $p_{nc}(\mathbf{x})$ is represented by a neural network. We use the term neural concepts to emphasize a key difference with traditional neurosymbolic systems such as DeepProbLog (Manhaeve et al. 2021), where neural predicates correspond to predefined symbolic relations with known intended meaning and are trained to recognize these concepts. In contrast, neural concepts in our setting do not have predefined target semantics. Instead, they are latent intermediate concepts whose meaning emerges through training, guided by the circuit structure and supervision signal. Consequently, NeTheR does not aim to preserve semantic interpretability of every concept. Rather, it preserves an explicit symbolic theory whose structure remains inspectable and revisable, while using latent neural concepts only where the existing symbolic vocabulary is insufficient.

In addition to the symbolic input space $\mathcal{X}_S$, we thus consider a neural input space $\mathcal{X}_N$, which consists of subsymbolic data such as images, multivariate time series, or other high-dimensional signals. Formally, $\mathcal{X}_N$ is a set of tensors, where each element $\mathbf{x} \in \mathcal{X}_n$ may represent, for example, a single image $\mathbf{x} \in \mathbb{R}^{H \times W \times C}$, a collection of multiple images $\mathbf{x} \in \mathbb{R}^{K \times H \times W \times C}$, or a multivariate time series $\mathbf{x} \in \mathbb{R}^{T \times d}$.

Figure 2 shows an example evaluation of an arithmetic circuit combining symbolic and neural probability functions.

Because the resulting arithmetic circuit consists entirely of differentiable operations, the neural network parameters can be trained end-to-end using gradient-based optimization. This enables learning latent features from indirect supervision, while leveraging the logical structure of the circuit to constrain and guide learning.

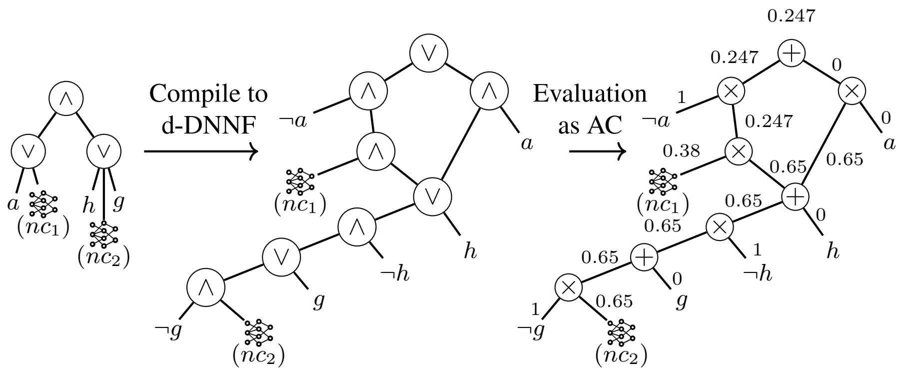

Figure 2. A logic formula is compiled into a d-DNNF and evaluated as an arithmetic circuit given the interpretation $\{a \rightarrow \mathit{false}, h \rightarrow \mathit{false}, g \rightarrow \mathit{false}\}$ with subsymbolic data feeding the neural networks, by which they evaluate to 0.38 and 0.65. These weights, and those of the symbolic input variables, are denoted above them. The weights propagate upwards, and those results are similarly denoted above the intermediate nodes.

2.5 *Theory Revision*

Theory revision studies how an existing logical theory can be modified to better explain observed examples while preserving as much prior knowledge as possible (Muggleton 1987; De Raedt 1992; Ourston and Mooney 1990; Mooney and Shavlik 2021). Rather than learning a theory from scratch, theory revision assumes an imperfect initial theory and seeks minimal modifications that improve predictive performance. Classical approaches revise theories through operations such as adding or removing literals, specializing or generalizing rules, or introducing new rules altogether (Mooney and Shavlik 2021).

In the classical setting, the available knowledge is typically divided into two parts (Mooney and Shavlik 2021): *background knowledge*, which is assumed to be correct and remains immutable throughout the revision process, and a *modifiable theory*, which is revised to better explain the observed examples.

A central mechanism in many theory revision and inductive logic programming systems is *predicate invention* (Muggleton 1987), which introduces new intermediate predicates that are not present in the original vocabulary and allows compact representations of useful abstractions in the data. A *neural concept* is a specialized case of a neural predicate: a nullary neural predicate without logical arguments, whose value is determined directly from the subsymbolic input.

3 Problem Setting

We consider a binary classification task defined over symbolic and subsymbolic data, in the presence of a possibly imperfect background model that the user may wish to revise.

Binary classification. Let $\mathcal{X} = \mathcal{X}_S \times \mathcal{X}_N$ denote the input space, consisting of a symbolic input space $\mathcal{X}_S$ and a subsymbolic input space $\mathcal{X}_N$. An input instance is denoted by $\mathbf{x} = (\mathbf{x}_S, \mathbf{x}_N) \in \mathcal{X}$, thus consisting of a symbolic and subsymbolic part. Let $\mathcal{Y} = \{0, 1\}$ denote the output space of Boolean labels. We assume the existence of an unknown target function $M^* : \mathcal{X} \to \mathcal{Y}$, which represents the true labeling mechanism. In practice, the true function M^* is not accessible. Instead, we are given a training set $E \subseteq \mathcal{X} \times \mathcal{Y}$ consisting of labeled instances. Each element $(\mathbf{x}_i, y_i) \in E$ contains an input instance $\mathbf{x}_i \in \mathcal{X}$ and its corresponding observed label $y_i \in \mathcal{Y}$. The label y_i may be provided by a human annotator, a measurement process, or another labeling system, and is assumed to be generated by the unknown target function M^*.

The goal of binary classification is to learn a model $M : \mathcal{X} \to \mathcal{Y}$ that approximates M^* and correctly predicts labels for both seen and unseen instances. Since M^* is unknown, the model must be learned from the labeled training set E. The hypothesis space $\mathcal{H}$ consists of all logic circuits whose leaf nodes are either symbolic literals or neural concepts, as defined in Section 2.

Each hypothesis $M \in \mathcal{H}$ defines a function $M : \mathcal{X} \to [0, 1]$, where inference is performed by evaluating the arithmetic circuit obtained from compiling the logic circuit as described in Section 2.3. This choice mirrors well-known neurosymbolic systems such as DeepProbLog (Manhaeve et al. 2021) and Scallop (Li et al. 2023), which use arithmetic circuits to compute probabilistic outputs during inference and learning. The output $M(\mathbf{x})$ represents the predicted probability of the positive class. During evaluation, this probabilistic output can be converted into a Boolean prediction by thresholding at 0.5 yielding a model $M : \mathcal{X} \to \mathcal{Y}$.

Additional knowledge. Our setting also comprises an initial, imperfect model $M' \in \mathcal{H}$ that serves as additional information to find M^*. This addition is motivated by the scenario wherein an expert already has an idea, albeit incorrect or incomplete, of the target model or a previously learned model, and aims to automatically revise it in a data-driven manner. The goal is thus to stay close to M' whilst increasing performance. We therefore also include a limit d_{max} on the allowed maximal distance between the input model M' and model M, measured using a distance function $d : \mathcal{H} \times \mathcal{H} \to \mathbb{R}_{\geq 0}$.

Summary. **Given** training set E, initial model $M' \in \mathcal{H}$, and distance bound d_{max}, we must **find** $M \in \mathcal{H}$ such that

$$\underset{M \in \mathcal{H}}{\operatorname{argmax}} \; F_1(M, M^*) \quad \text{s.t. } d(M, M') \leq d_{max}, \tag{3}$$

where

$$F_1(M, M^*) = \mathbb{E}_{\mathbf{x} \sim D}[F_1\big(M(\mathbf{x}), M^*(\mathbf{x})\big)]$$

denotes the expected F_1-score of M compared to M^*, with respect to input distribution $\mathcal{D}$ over $\mathcal{X}$. We use the F_1-score because the input theory is intended to distinguish the positive class from the remaining classes, making performance on the positive class more important. If both classes are equally important, the F_1-score can be replaced by balanced accuracy in both problem setting and the following method. A natural choice for d is the minimal number of modification steps required to obtain M from M'. The types of modifications we consider are discussed in the next section.

4 Our Approach: NeTheR

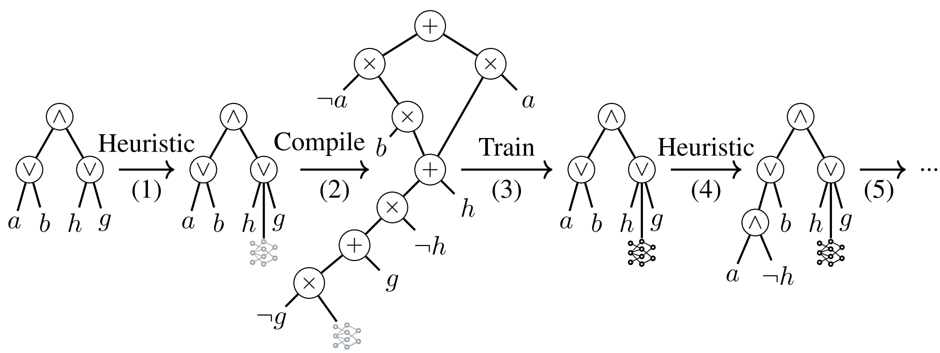

Figure 3. Example of the revision process by NeTheR. (1) An untrained neural concept is added; (2) The result is compiled to an arithmetic circuit; (3) This circuit allows us to efficiently compute probabilities and is end-to-end differentiable, such that the neural concept(s) are trained as part of the logical circuit; (4) Once trained, NeTheR performs again a new modification which may add a new symbolic literal; (5) This cycle repeats until the maximum number of modifications is reached or until modifications would decrease performance. An important task is then to efficiently identify high-impact modifications: where do we insert a new neural concept or symbolic literal; or what existing concepts should we remove?

We now introduce *NeTheR*, a greedy theory revision approach that incrementally improves a logic circuit through the incorporation of new symbolic literals and neural concepts, inspired by classical symbolic theory revision. The goal is to identify a sequence of structural modifications that improves predictive performance while remaining close to the original model. An overview is shown in Figure 3, where both a neural concept and a symbolic literal are introduced to refine the formula.

We formalise theory revision as an optimisation problem over circuit nodes and their structural replacements. Let $M^{(0)} = M'$ denote the initial logic circuit, and let $\mathcal{N}^{(t)}$ denote the set of nodes in the circuit $M^{(t)}$ at revision step t.

A modification at node n replaces the subcircuit rooted at n with a new subcircuit n', producing a revised model $M^{(t+1)} = M^{(t)}[n \leftarrow n']$. Our objective is to construct a sequence of revisions $M^{(0)} \to M^{(1)} \to \cdots \to M^{(T)}$ that maximises predictive performance while limiting deviation from the original model $M^{(0)}$.

Because the space of possible revision sequences is combinatorial, *NeTheR* adopts a greedy strategy that selects, at each step, the locally optimal modification according to a performance objective subject to a proximity constraint. Each greedy step solves:

$$M^{(t+1)} = M^{(t)}[n \leftarrow n'] \text{ with } \underset{\substack{n \in \mathcal{N}^{(t)} \\ n' \in \mathcal{M}(n)}}{\operatorname{argmax}} F_1\big(M^{(t)}[n \leftarrow n'](X), Y\big) \text{ and } t < d_{\max}. \quad (4)$$

where $\mathcal{M}(n)$ denotes the set of admissible replacement subcircuits at node n.

4.1 Modification Types

Let M be a logic circuit and n a node in this circuit. Theory revision operates by locally modifying subcircuits rooted at n. These modifications fall into two categories:

- **Generalisation**, which makes the model less restrictive and may increase the set of inputs classified as positive. Structurally, generalisation is achieved by replacing n with *true* (removal) or by introducing a new node m in disjunction, $n \vee m$.
- **Specialisation**, which makes the model more restrictive and may decrease the set of inputs classified as positive. Structurally, specialisation is achieved by replacing n with *false* (removal) or by introducing a new node m in conjunction, $n \wedge m$.

To determine which modifications are most promising, we analyse the influence of each node through intervention. We consider two types of intervention. Either a node n is replaced by *true*, $M[n \leftarrow \mathit{true}](x)$, or n is replaced by *false*, $M[n \leftarrow \mathit{false}](x)$. These intervention models allow us to identify the examples whose classification depends on node n, which we refer to as the influence set:

- **Generalisation influence set**

  $$E^{(n)}_{\text{gen}} = \{(x, y) \in E \mid M(x) = 0 \;\wedge\; M[n \leftarrow \mathit{true}](x) = 1\}. \quad (5)$$

  These are the examples that are not covered by M, but can be covered by generalising node n.
- **Specialisation influence set**

  $$E^{(n)}_{\text{spec}} = \{(x, y) \in E \mid M(x) = 1 \;\wedge\; M[n \leftarrow \mathit{false}](x) = 0\}. \quad (6)$$

  These are the examples that are covered by M, but not anymore when specialising node n.

These influence sets identify exactly the examples whose classification can be changed through modification of node n, and are used to learn new symbolic literals and neural concepts. We now formalise the three modification types.

1. **Removal of a literal.**
   The literal n is replaced with a constant:

   $$n' \in \{\mathit{true}, \mathit{false}\}.$$

   Replacing n with *true* performs generalisation, while replacing it with *false* performs specialisation.

2. **Symbolic literal insertion.**
A new leaf node m representing a symbolic literal is introduced and combined with n:
$$n' = \begin{cases} n \lor m & \text{(generalisation)} \\ n \land m & \text{(specialisation).} \end{cases}$$
The literal of leaf node m is learned from data using a decision tree of depth 1 (i.e., a decision stump) trained on the corresponding influence set. For generalisation, the stump is trained on $E^{(n)}_{\text{gen}}$ to identify conditions under which the prediction should become positive. For specialisation, it is trained on $E^{(n)}_{\text{spec}}$ to identify conditions under which the prediction should become negative.
Decision stumps provide sufficient expressivity to generate Boolean atoms over both categorical and continuous variables, as explained in Section 2.1.
3. **Neural concept insertion.**
A new leaf node nc, representing an invented neural concept, is introduced and combined with n:
$$n' = \begin{cases} n \lor nc & \text{(generalisation)} \\ n \land nc & \text{(specialisation).} \end{cases}$$
Unlike symbolic literals, whose truth values are directly determined by the symbolic input, the value of nc is computed by a differentiable neural network. The network operates on the available subsymbolic input (e.g., images or time series) and outputs the probability that the invented predicate holds. This probability is treated as the value of a probabilistic literal and is propagated through the arithmetic circuit during inference, allowing the learned neural representation to directly influence symbolic reasoning.
The neural network is trained on the corresponding influence set. For generalisation, it is trained on $E^{(n)}_{\text{gen}}$ to recognise additional positive patterns that should satisfy the revised theory. For specialisation, it is trained on $E^{(n)}_{\text{spec}}$ to recognise patterns that should be excluded. During this optimization, the symbolic structure of the revised circuit remains fixed, while the parameters of the newly introduced neural concept are learned by gradient-based optimization.
The introduced neural concepts represent properties that are not explicitly available in the symbolic vocabulary, but must instead be inferred from subsymbolic observations. Unlike traditional neurosymbolic systems such as DeepProbLog (Manhaeve et al. 2021), where neural predicates correspond to predefined semantic concepts, the neural concepts introduced by NeTheR have no predefined meaning. Their semantics emerge through the interaction between symbolic reasoning and neural learning: the arithmetic circuit determines where a neural concept is introduced and provides the supervision signal, while the neural network learns a representation whose output probabilities improve the overall symbolic theory. Consequently, NeTheR extends classical theory revision by allowing revisions that jointly modify the symbolic structure and introduce learned neural concepts grounded in subsymbolic data.

NeTheR instantiates invented concepts as differentiable neural networks. Depending on the application domain, different neural architectures can be employed, such as convolutional neural networks for images, recurrent neural networks for sequential data, or temporal convolutional networks for time-series data. More generally, any model that provides a calibrated probability for the invented concept could be integrated into the arithmetic circuit. Replacing the neural network with a non-neural model would yield a learned probabilistic concept rather than a neural concept, which we consider to be outside of the neurosymbolic focus of this work.

To ensure a structured and interpretable hypothesis space, neural concepts cannot be directly combined with other neural concepts. For example, expressions such as $nc_1 \wedge nc_2$ and $nc_1 \vee nc_2$ are not allowed, while structured combinations such as $(x \vee nc_1) \wedge nc_2$ remain valid.

This restriction ensures that the number of candidate modifications grows linearly with circuit size. For a circuit with l symbolic literals, n neural concepts, and i inner nodes, the number of candidate modifications is at most $3l + 2i + n + 2$ (see Appendix A). Finally, if no candidate modification improves performance, the current model is considered locally optimal and the revision process terminates. Following the formulation introduced in Section 2.5, the classical theory revision setting can be recovered by restricting the set of admissible revision locations. Designated portions of the logical theory can thereby be treated as immutable background knowledge, while revisions are only permitted on the remaining logical subcircuits corresponding to the modifiable theory.

4.2 Modification Selection

When revising a logic circuit, symbolic and neural modifications differ fundamentally in how their impact can be evaluated. For symbolic revisions, the effect of a modification can be determined exactly prior to applying it. This is because symbolic modifications introduce only deterministic circuit structure, and the resulting model can be evaluated tractably using standard arithmetic circuit inference.

In contrast, inserting a neural concept introduces a component whose behavior depends on learnable parameters. While the circuit structure determines how the new node nc influences the model, its probability function $p_{nc}(x)$ is represented as a neural network with initially unknown parameters. These parameters must be learned from data through training. As a result, the performance of the modified model $M[n \leftarrow n']$ cannot be determined exactly without performing this training procedure.

Consequently, evaluating candidate neural revisions is significantly more computationally expensive than evaluating symbolic revisions, as each candidate requires training a neural network to determine its impact. This makes exhaustive evaluation of all possible neural modifications infeasible in practice. Therefore, enabling tractable revision requires estimating the potential impact of neural modifications prior to training, allowing promising revisions to be identified efficiently without incurring the full computational cost of neural optimization.

4.2.1 Upper and lower bounds. Let n be a candidate insertion node. The sets $E^{(n)}_{\text{gen}}$ and $E^{(n)}_{\text{spec}}$, defined above in equations 5 and 6 respectively, characterise the examples whose classification can be changed by generalising or specialising node n, respectively. Since the new neural concept nc is initially untrained, its exact predictions on the influence set are unknown. However, we can derive bounds on the achievable performance by considering upper and lower bound probability functions p^* and $p_\perp$.

- *Best case (B).* The neural concept correctly identifies all examples in $E^{(n)}_{\text{gen/spec}}$:

$$p^*(x) = y \quad \text{for all } (x, y) \in E^{(n)}_{\text{gen/spec}}. \tag{7}$$

- *Worst case (W).* The neural concept makes incorrect predictions on all examples:

$$p_\perp(x) = 1 - y \quad \text{for all } (x, y) \in E^{(n)}_{\text{gen/spec}}. \tag{8}$$

These probability functions define the best-case and worst-case modified subcircuits n^* and $n_\perp$, respectively. The corresponding performance bounds are:

$$B = F_1\big(M[n \leftarrow n^*](X), Y\big), \quad W = F_1\big(M[n \leftarrow n_\perp](X), Y\big). \tag{9}$$

By construction, the performance of any neural concept inserted at node n is bounded by:

$$W \;\leq\; F_1\big(M[n \leftarrow n'](X), Y\big) \;\leq\; B. \tag{10}$$

These bounds allow us to estimate the potential benefit and risk of inserting a neural concept without training the neural network.

Selecting the modification with maximal best-case score B is optimistic and favours expressive revisions, analogous to model selection criteria such as AIC and BIC (Akaike 1998; Schwarz 1978). In contrast, selecting the modification with maximal worst-case score W is conservative and favours safer symbolic revisions.

4.2.2 Sharpe ratio. To consider both the best and worst case scenarios simultaneously, we create a more sophisticated heuristic based on the *Sharpe ratio* (Pav 2021). The Sharpe ratio S is a widely used metric in finance to assess the risk-adjusted performance of an investment p. It is derived from the statistical t-test and is mathematically defined as the difference between R_p, which is the expected return of the investment p, and R_f, which is the return from a theoretical risk-free investment f. The denominator σ_p is the standard deviation of p's excess returns, quantifying the variability in p's performance. I.e., $S = (R_p - R_f)/\sigma_p$. In essence, this formula highlights how much excess return is achieved per unit of risk taken. A higher Sharpe ratio S indicates a better risk-adjusted performance. As the metric is particularly useful for comparing investments with varying levels of risk, it is frequently used in the context of multi-armed bandit problems (Cassel et al. 2018; Khurshid et al. 2025; Xi et al. 2021).

While the Sharpe ratio is traditionally used to quantify the risk-adjusted return of an investment, we use it to quantify the risk-adjusted utility of a candidate neural revision. In both settings, the numerator represents the expected gain relative to a baseline, while the denominator captures the uncertainty associated with that gain. In our setting, the expected return corresponds to the predicted performance improvement of a neural modification over the current model, and the uncertainty reflects how reliably this improvement can be estimated before training. The Sharpe ratio therefore prioritizes revisions that offer a favorable trade-off between expected improvement and predictive uncertainty. An alternative risk-adjusted criterion is the Sortino ratio, which replaces the standard deviation by the downside deviation and therefore penalizes only outcomes below the risk-free baseline (Sortino and Price 1994). In principle, this encourages more optimistic exploration by discounting unexpectedly good outcomes. Similar to the investment p, we do not know the performance of a neural concept prior to training and only know its best and worst case impact. In other words, we can use the Sharpe ratio S to objectively trade off the risk (W) and reward (B) of each circuit modification, and select the best modification as the one with the highest S.

Using the distribution X_{nc} to denote the performance of neural concept nc in a specific location of the logic circuit, we interpret X_{nc} as the distribution over all possible trained outcomes of the modified model i.e., over all attainable F_1 scores between the worst-case bound W and the best-case bound B.

Its expectation $\mathbb{E}[X_{nc}]$ serves as a substitute for R_p, while the standard deviation $\sigma[X_{nc}]$ replaces σ_p. Finally, the risk-free rate R_f corresponds to the F_1-score of the best modification with a precisely known impact: either the removal of a literal or neural concept, the addition of a new symbolic literal, or performing no modification at all:

$$S = \frac{\mathbb{E}[X_{nc}] - R_f}{\sigma[X_{nc}]}. \tag{11}$$

The distribution X_{nc} depends on both the neural network's architecture and the classification task. In our empirical evaluation, we assume that X_{nc} is a two-point weighted random variable whose mean is $\mu = \alpha B + (1-\alpha)W$ and variance is $Var(X_{nc}) = \alpha(B-\mu)^2 + (1-\alpha)(W-\mu)^2$, and we use these as parameters for a shifted normal distribution. This results in

$$S = \frac{\alpha B + (1-\alpha)W - R_f}{\sqrt{\alpha((1-\alpha)B - (1-\alpha)W)^2 + (1-\alpha)(\alpha W - \alpha B)^2}} \tag{12}$$

where $\alpha \in (0,1)$ shifts the distribution closer to the best case when $\alpha > 0.5$. This equation assumes the presence of risk, i.e., $B \neq W$. Risk-free modifications are only selected when the best S is negative, i.e., when the expected F_1-score $\mathbb{E}[\mathbf{X}_{nc}]$ is worse than the best risk-free modification. A full example of a single modification selection is shown in Appendix B.

The proposed heuristic estimates the utility of inserting a neural concept prior to training, based solely on structural bounds. Consequently, the selected modification is not guaranteed to remain optimal after the neural concept has been trained, since training changes the effective decision boundary and may alter the relative utility of subsequent revisions. Our approach therefore relies on the assumption that it is easier to identify where in the symbolic theory a neural concept is likely to be beneficial than to accurately predict how much that neural concept will improve performance after training. The dynamic update of α partially compensates for this mismatch by continuously calibrating the expected performance of future neural insertions using previously observed outcomes.

4.2.3 Dynamic Sharpe ratio. Instead of choosing a fixed value for α, we determine it dynamically using an exponential smoothing scheme: after training a neural network nc, we adjust α such that the estimated $\mathbb{E}[X_{nc}]$ better matches nc's actual performance. Denoting α_t as the correct value according to the neural network's performance, we move α closer to this value by updating it $\alpha \leftarrow (\alpha + \alpha_t)/2$. In addition to the periodic updates of α, we also choose a more informed initial value by randomly selecting k insertion modifications and evaluating the predicted performance with its actual performance. We select a modification with worst case W and best case B and train the network, resulting in F_1-score x. α is then $\frac{x-W}{B-W}$, showing how close we are to the best case. When $k > 1$, α is the average of all k estimates.

By dynamically adjusting α, the proposed heuristic provides a more accurate estimate of risk and captures performance trends across different scenarios. In contrast, the strategies that always select the worst-case performance W, the best-case performance B, or a fixed value $\alpha = 0.5$ constitute trivial alternatives. Always selecting W systematically undervalues the neural concept, leading it to be consistently rejected in favor of symbolic revision, as it is predicted to worsen the theory. Conversely, always selecting B overvalues the neural concept, causing it to be chosen in all cases. Fixing $\alpha = 0.5$ similarly fails to adapt to changing performance conditions. Using the dynamic variant of the Sortino ratio also overvalues neural concepts in less favorable situations. The ablation study in Appendix C.1 confirms that the dynamic Sharpe-ratio-based selection outperforms these baselines.

4.3 Algorithm

We now discuss the outline of NeTheR using Algorithm 1. First, we determine a suitable, initial α parameter (line 3) to better estimate the potential impact of each possible neural concept, as explained in the previous paragraph. Then, we iteratively apply the modification with the highest estimated Sharpe ratio (line 6 and 7) until the maximum distance is reached (line 5), or until the next best modification is to make no change at all (line 8). Note that it is expensive to compute distance $d(M, M')$ in equation 3, so we approximate it by counting the number of performed modifications, potentially overestimating the true distance and thus stopping too early. After this selection, we recompile the theory into a d-DNNF representation, and perform end-to-end parameter learning to update the neural network weights in case the modification added a neural concept (line 9). Once the learning process is complete, we can verify whether the estimated performance was correct, and update α accordingly to improve future estimates (line 9). Finally, if the F_1-score improved the best found result, we update M and continue to further modify the result (line 10). In case the F_1-score did not improve, M did not change and the while loop repeats with the next best untried modification, using the best model found so far. Finally, we return the best found model (line 11).

NeTheR can be viewed as a greedy block coordinate ascent procedure (Wright 2015) over two coupled optimization variables: the symbolic structure of the theory and the parameters of the neural concepts. At each iteration, the symbolic structure is updated by selecting a single revision using the proposed Sharpe-ratio heuristic. If the selected revision introduces a neural concept, only the parameters of this newly introduced concept are subsequently optimized, while previously learned neural concepts remain fixed. This alternating optimization provides an efficient approximation to joint structure and parameter learning, but does not guarantee convergence to a globally optimal solution.

Algorithm 1 NeTheR

Input:
Imperfect logic circuit M', Maximum distance d_{max},
Training and validation set $T, V \subseteq E$, Number of modifications to initialize k
Output: Revised model M
$\alpha \leftarrow$ initialise_alpha(M', k)
$M \leftarrow M'$
while $d(M', M) \leq d_{max}$ **do**
    $\mathcal{M} \leftarrow$ all untried modifications $(n \leftarrow n')$ for M
    $M'' \leftarrow argmax_{M[n \leftarrow n'] | (n,n') \in \mathcal{M}}\ S(M[n \leftarrow n'], \alpha)$
    if $M'' = M$ **then** *break*
    if M'' includes a neural concept **then** $train(M'', T)$, update α
    if $F_1(M'', V) > F_1(M, V)$ **then** $M \leftarrow M''$
return M

Training the model. When inserting a neural concept, we train the underlying neural network in an end-to-end fashion with the rest of the logic circuit, using indirect supervision. For example, if our logic circuit is $M = nc_1 \wedge (x \vee nc_2)$, with nc_1 and nc_2 neural concepts and x a symbolic literal, then we train M using our training dataset; there is no direct label for the neural network. Since the task is binary classification, the neural concepts are trained using the binary cross-entropy loss with logits (`BCEWithLogitsLoss` in PyTorch), which combines a sigmoid activation with the binary cross-entropy objective in a numerically stable formulation. By compiling the logic circuit into d-DNNF prior to training its arithmetic version, we have the benefit of probabilistic semantics (cf. Figures 2 and 3, and Sections 2.3 and 2.4). Integrating a new neural concept enables the logic circuit to capture additional useful features. This is particularly advantageous when the subsymbolic data contains information not present in symbolic form, while also increasing robustness against noise in the symbolic data as the inserted neural concept may mitigate inconsistencies.

During training, NeTheR only updates the parameters of the newly inserted neural network and keeps the other parameters frozen. From an optimization perspective, this corresponds to updating only the newly introduced parameter block after each structural revision, rather than jointly optimizing all neural concepts after every modification. Joint optimization could in principle converge to a better local optimum by accounting for interactions between neural concepts, but would substantially increase the computational cost of each revision step. We evaluate this alternative in the ablation study presented in Appendix C.2. The results show that joint optimization does not improve classification performance on the evaluated datasets, while substantially increasing runtime. We therefore freeze previously learned neural concepts throughout the empirical evaluation, as this provides a favorable trade-off between computational efficiency and predictive performance.

5 Evaluation

We empirically evaluate NeTheR on relevant benchmarks, assessing its effectiveness at solving the revision problem (cf. Section 3) compared to alternative approaches. In the theoretical setting, the target model M^* is unknown and must be approximated using labeled data. For the purpose of experimental evaluation, we will define a ground-truth target model M^* and generating labeled instances from it. This allows us to quantitatively assess how well the revised model approximates the true underlying model.

We investigate two scenarios: a structurally informed scenario where the initial model M' is structurally close to the target model M^*, and a structurally uninformed scenario where this is not the case. The structurally informed setting evaluates NeTheR under its intended assumptions: namely, that the initial theory differs from the target by only a small number of local revisions. This controlled setup allows us to evaluate whether the proposed search strategy can recover such revisions: it assesses the effectiveness of theory revision, rather than to serve as a generic benchmark for neurosymbolic learning methods. The structurally uninformed setting complements this by considering a realistic hybrid workflow, in which an initial symbolic theory is first learned automatically from data as a decision tree and subsequently refined using NeTheR. This setting evaluates whether local theory revision remains beneficial when the initial model is only a coarse approximation of the target, reflecting practical scenarios.

5.1 Experimental Setup

We consider 9 open-source benchmark datasets, as listed in Table 1, with more details included in Appendix D.

Six of those datasets have images as subsymbolic data, whilst three datasets demonstrate our method's ability to also operate on non-image data, such as music and time series.

The open-source datasets do neither include an imperfect initial model M', nor a target model M^* from which we can extract a structurally close M'. Hence, we generate for each dataset 24 logic circuits M^*, resulting in 216 binary classification problem instances in total. From M^* we obtain an initial model M' that is imperfect but structurally close, by systematically removing variables, lowering the F_1-score until it is in the range of 0.6 to 0.9. Importantly, we also remove these variables from the training dataset, to simulate the setting one encounters in practice where this data is not present. This means NeTheR

Table 1. The 9 open-source datasets that are used in the experimental evaluation, with d_S denoting the number of symbolic features.

Dataset	#instances	d_S	type of subsymbolic data
Austin Texas Housing (ATH) (Pierce 2021)	5508	37	image
AWA2 (Xian et al. 2019)	5000	85	image
CelebA (Liu et al. 2015)	10000	40	image
CUB (Wah et al. 2011)	11788	312	image
derm7pt (Kawahara et al. 2019)	1011	13	image
FMA (Defferrard et al. 2017)	9217	14	audio + echonest features
Motifs, based on TSMD-bench (Van Wesenbeeck et al. 2024)	5000	180	time series
Pascal VOC (Everingham et al. 2010)	17125	20	image
StarLightCurves (Rebbapragada et al. 2009)	9236	21	time series

must revise M' using only the subsymbolic features, and the symbolic features already present in M'.

For the experiment without structural information, we use as initial model M' a decision tree that is learned for each problem instance. After filtering on imperfect initial models M', i.e., those with an F_1-score below 0.9, we obtain 171 instances. These represent an expert's imprecise knowledge that is not necessarily structurally close to M^*. Similar to the experiment with structural information, we restrict the symbolic features to only those present in M'. More information on the generation of these problem instances is given in Appendix D. Appendix G shows an instance of the problem for both the structurally informed and uninformed experiment, together with the corresponding revised model by NeTheR. Appendix E includes an additional, similar, experiment on the derm7pt dataset (Kawahara et al. 2019), wherein we use the existing dataset labels instead of M^*.

As our distance function d tracks the number of modifications, we set d_{max} to the number of systematic removals from M^* to M'. Each dataset was split into 80% training, 10% validation and 10% test data. For NeTheR, we use $k = 3$ to estimate an initial α, and freeze the parameters of previously added neural concepts when training.

Used neural networks. Depending on the type of subsymbolic data, we use a different type of neural network to parameterize the neural concepts. For images, we use a pre-trained ResNet-50 and train a 6-layer multi-layer perceptron (MLP) concatenated to the last fully connected ResNet-50 layer; for music (FMA dataset), we only use and train the MLP; and for time series (StarLightCurves and Motifs), we use and train the InceptionTime network (Fawaz et al. 2020). All of these are trained for 50 epochs with patience set to 5. Sklearn is used to learn the decision stump in case of a new symbolic literal.

5.2 Baseline Comparison

To evaluate the effectiveness of NeTheR, we compare against the following five baseline methods:

CMR A state-of-the-art concept-based model that was initialised with M', and that was allowed to learn 20 additional rules (Debot et al. 2024).

And Or A simple but very general extension of M': $(M' \vee nc_1) \wedge nc_2$, with nc new neural concepts.

Or And A simple but very general extension of M': $(M' \wedge nc_1) \vee nc_2$, with nc new neural concepts.

NN A single neural network exploiting only subsymbolic data. For each dataset, we use the same neural network architecture as used to parameterize the neural concepts, but without the logic circuit.

MLP+NN A multimodal network combining the single neural network with an MLP to also exploit symbolic data (Ahsan et al. 2020; Gessert et al. 2020).

Classical theory revision systems were omitted as baselines because they operate exclusively on symbolic inputs, and are thus unable to introduce concepts derived from subsymbolic data. Information on the used computing infrastructure is found in Appendix F.

The *NN* approach learns a single neural network, and takes on average 6 minutes. The remaining baselines, *CMR*, *And Or*, *Or And*, and *MLP+NN* each learn two networks, and complete on average in 9, 7, 8, and 12 minutes respectively. In comparison, NeTheR trains an average of 1.5 neural networks during the search phase, and another 2.2 to estimate parameter $\alpha^{\dagger}$. Again on average, NeTheR completes the full revision process in approximately 22 minutes: 12.5 minutes are spent estimating an initial α, 5 minutes are spent training neural networks during the search phase, 5.5 minutes are spent enumerating the possible modifications and compiling the revised circuit took less than a second. In case a sufficient estimate for α is available, the initial step of the algorithm can be avoided entirely. Finally, one could use cheaper proxy models or train the sampled neural concepts for only a small number of epochs to obtain a rough initial calibration. These alternatives would reduce the initialization overhead, but may also make early revision decisions less reliable. Exploring this trade-off between calibration cost and search quality is an interesting direction for future work.

Table 2 and 3 summarize the numerical results of the structurally informed and uninformed experiment respectively, by providing for each dataset the mean improvement of F_1-score over the initial model M'. The F_1-score for M' itself is provided in Table 4. Figure 4 contains the critical difference diagrams for

†Even though we use k=3 when evaluating NeTheR, some instances have fewer locations to insert a neural network such that the average k is lower.

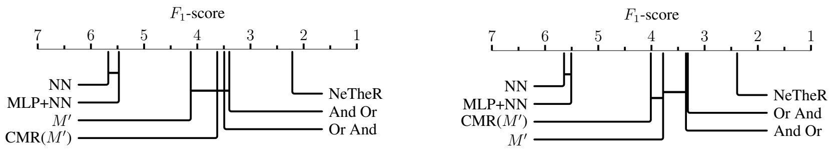

(a) M' with structural information

(b) M' without structural information

Figure 4. Critical difference diagrams (Demšar 2006; Benavoli et al. 2016), demonstrating the effectiveness of NeTheR. It plots the average rank (closer to 1 is better) and connects with a horizontal line those methods whose performance is not significantly different. We include input model M'.

both experiments, showing that NeTheR clearly outperforms the other approaches. Interestingly, the multimodal neural network *MLP+NN* does not perform significantly better than the single neural network *NN*. This indicates that the additional complexity does not necessarily translate to better results, because the subsymbolic data may provide a sufficient signal to replace the symbolic features. We also observe that both of these methods frequently perform worse than M'. This illustrates well that starting from an existing imperfect model M' has obvious performance benefits. The other three methods, *CMR*, *And Or*, and *Or And*, do exploit the existing information from M'. Still, their performance often significantly lags behind NeTheR's. We believe this is because NeTheR is more robust against bad performing neural concepts through a more fine-grained placement. In the other methods neural networks have a central role, heavily influencing the performance: for *And Or* and *Or And* this is obvious, in case of *CMR*, a neural predictor is key in deciding which logical rule determines the prediction. This also explains why NeTheR is more performant in data-poor settings compared to the other methods, as shown in Appendix C.3.

Table 2 and 3 summarize the numerical results of the structurally informed and uninformed experiment respectively, by providing for each dataset the mean improvement of F_1-score over the initial model M'. The F_1-score for M' itself is provided in Table 4.

To understand the contribution of each modification type, we analysed the cumulative improvement in F_1-score attributable to symbolic insertions, neural concept insertions, and removal operations throughout the greedy revision process. For each run, we summed the improvement obtained immediately after every accepted modification of a given type and averaged these cumulative contributions across all runs. The results are shown in Table 5.

Across all setting, split and dataset configurations, symbolic revisions show a consistent, positive mean improvement, with an average contribution to the F_1-score ranging from 0.01 to 0.04, with standard deviations ranging from 0.04 to 0.08. The behavior of removal operations is very similar. Together, these findings indicate that symbolically refining and pruning the theory forms a stable and reliable component of the revision process by NeTheR, irrespective of the initialization strategy or dataset type.

Table 2. Comparison with other methods, demonstrating the effectiveness of NeTheR when M' is structurally informed. The values are the mean differences in F_1-score between the learned model M and the input model M', i.e., $F_1(M(x), M^*(x)) - F_1(M'(x), M^*(x))$, aggregated per dataset. Higher is better. The F_1-scores for the input model M' are shown in Table 4.

Datasets	Methods					
	NeTheR	And Or	Or And	NN	MLP+NN	CMR
ATH	**+0.10±0.1**	-0.13±0.2	-0.15±0.2	-0.32±0.2	-0.32±0.3	+0.00±0.1
AWA2	+0.10±0.1	**+0.13±0.1**	+0.12±0.1	+0.04±0.1	-0.07±0.1	+0.10±0.1
CelebA	**+0.11±0.1**	+0.04±0.1	+0.04±0.1	-0.15±0.2	-0.25±0.3	+0.00±0.1
CUB	**+0.10±0.1**	-0.02±0.1	-0.02±0.1	-0.28±0.3	-0.38±0.4	-0.01±0.1
derm7pt	**+0.07±0.1**	-0.26±0.3	-0.31±0.3	-0.58±0.3	-0.56±0.3	-0.06±0.1
FMA	**+0.08±0.1**	+0.04±0.1	+0.04±0.1	-0.42±0.2	-0.05±0.2	-0.05±0.1
motifs	**+0.07±0.1**	-0.09±0.2	-0.13±0.3	-0.61±0.2	-0.63±0.2	-0.06±0.2
Pascal VOC	+0.15±0.1	**+0.17±0.1**	**+0.17±0.1**	+0.06±0.2	+0.07±0.2	+0.14±0.1
StarLightCurves	+0.08±0.1	-0.15±0.4	+0.04±0.3	-0.53±0.3	-0.10±0.4	**+0.12±0.1**

Table 3. Comparison with other methods, demonstrating the effectiveness of NeTheR when M' is structurally uninformed. The values are the mean differences in F_1-score between the learned model M and the input decision tree M', i.e., $F_1(M(x), M^*(x)) - F_1(M'(x), M^*(x))$, aggregated per dataset. Higher is better. The F_1-scores for the input model M' are shown in Table 4.

Datasets	Methods					
	NeTheR	And Or	Or And	NN	MLP+NN	CMR
ATH	**+0.12±0.1**	-0.08±0.2	-0.03±0.1	-0.4±0.3	-0.38±0.2	-0.28±0.2
AWA2	**+0.08±0.1**	+0.02±0.1	+0.02±0.1	-0.02±0.1	-0.13±0.1	+0.06±0.1
CelebA	**+0.07±0.1**	+0.05±0.1	+0.04±0.1	-0.13±0.2	-0.25±0.3	-0.05±0.2
CUB	**+0.07±0.1**	-0.02±0.1	+0.02±0.1	-0.26±0.3	-0.36±0.4	-0.23±0.2
derm7pt	**+0.05±0.1**	-0.02±0.1	-0.02±0.1	-0.64±0.3	-0.64±0.3	-0.14±0.1
FMA	-0.03±0.2	**+0.01±0.1**	**+0.01±0.1**	-0.48±0.2	-0.13±0.3	-0.05±0.1
motifs	-0.05±0.3	-0.19±0.4	-0.18±0.4	-0.47±0.3	-0.54±0.3	**+0.00±0.3**
Pascal VOC	**+0.16±0.1**	+0.11±0.1	+0.10±0.1	+0.06±0.2	+0.07±0.2	**+0.16±0.1**
StarLightCurves	-0.10±0.3	+0.06±0.2	+0.01±0.3	-0.51±0.2	-0.12±0.3	**+0.12±0.1**

Neural concept insertion exhibits larger variability, with standard deviations ranging from 0.06 to 0.18. On all image datasets, neural revisions provide a mean improvement to the F_1-score, indicating that the introduced neural concepts successfully capture information unavailable in the symbolic representation while benefiting from pretrained visual feature extractors. In contrast, on the non-image datasets, neural revisions contribute negatively on the test set (-0.09 and -0.04 for the structurally informed and structurally uninformed settings respectively), while contributing positively on the validation set (+0.15 and +0.12). This discrepancy suggests that neural revisions are less robust when the neural network must be trained from scratch, which is the case for non-image data but not for image data. This causes the greedy search to select revisions that appear beneficial on the validation set but generalize poorly to unseen data.

Table 4. Average F_1-score of input model M' for each dataset. M'_1 is the model used for the structurally informed experiment, while M'_2 is the learned imperfect decision tree that is used for the uninformed experiment.

Dataset	$F_1(M'_1(x), M^*(x))$	$F_1(M'_2(x), M^*(x))$
ATH	0.76±0.1	0.80±0.1
AWA2	0.77±0.1	0.84±0.1
CelebA	0.78±0.1	0.74±0.1
CUB	0.80±0.1	0.78±0.2
derm7pt	0.77±0.1	0.81±0.1
FMA	0.74±0.1	0.78±0.1
motifs	0.75±0.1	0.64±0.2
Pascal VOC	0.74±0.1	0.70±0.2
StarLightCurves	0.77±0.1	0.75±0.1

Table 5. Average cumulative F1 contribution ($\mu_{\pm\sigma}$) of each accepted modification type during the revision process.

Setting	Split	Datasets	Symbolic	Neural	Removal
Structurally informed	Test	Non-image	$+0.01_{\pm 0.05}$	$-0.09_{\pm 0.18}$	$+0.02_{\pm 0.07}$
	Test	Image	$+0.02_{\pm 0.08}$	$+0.03_{\pm 0.06}$	$+0.04_{\pm 0.09}$
	Test	All	$+0.02_{\pm 0.07}$	$-0.01_{\pm 0.13}$	$+0.04_{\pm 0.08}$
	Validation	Non-image	$+0.01_{\pm 0.04}$	$+0.15_{\pm 0.13}$	$+0.02_{\pm 0.05}$
	Validation	Image	$+0.03_{\pm 0.07}$	$+0.04_{\pm 0.06}$	$+0.04_{\pm 0.08}$
	Validation	All	$+0.03_{\pm 0.07}$	$+0.07_{\pm 0.11}$	$+0.04_{\pm 0.08}$
Structurally uninformed	Test	Non-image	$+0.03_{\pm 0.08}$	$-0.04_{\pm 0.18}$	$+0.02_{\pm 0.06}$
	Test	Image	$+0.02_{\pm 0.05}$	$+0.06_{\pm 0.08}$	$+0.01_{\pm 0.04}$
	Test	All	$+0.02_{\pm 0.06}$	$+0.03_{\pm 0.13}$	$+0.01_{\pm 0.05}$
	Validation	Non-image	$+0.04_{\pm 0.08}$	$+0.12_{\pm 0.16}$	$+0.02_{\pm 0.05}$
	Validation	Image	$+0.02_{\pm 0.05}$	$+0.06_{\pm 0.08}$	$+0.01_{\pm 0.04}$
	Validation	All	$+0.02_{\pm 0.06}$	$+0.08_{\pm 0.12}$	$+0.02_{\pm 0.04}$
Combined	Test	Non-image	$+0.02_{\pm 0.07}$	$-0.07_{\pm 0.18}$	$+0.02_{\pm 0.06}$
	Test	Image	$+0.02_{\pm 0.07}$	$+0.04_{\pm 0.08}$	$+0.03_{\pm 0.07}$
	Test	All	$+0.02_{\pm 0.07}$	$+0.01_{\pm 0.13}$	$+0.03_{\pm 0.07}$
	Validation	Non-image	$+0.02_{\pm 0.06}$	$+0.14_{\pm 0.14}$	$+0.02_{\pm 0.05}$
	Validation	Image	$+0.03_{\pm 0.06}$	$+0.05_{\pm 0.07}$	$+0.03_{\pm 0.07}$
	Validation	All	$+0.03_{\pm 0.06}$	$+0.08_{\pm 0.11}$	$+0.03_{\pm 0.06}$

Overall, these results demonstrate that the improvements achieved by NeTheR arise from complementary mechanisms. Symbolic revisions provide small but consistently reliable improvements by correcting the logical structure, whereas neural concept invention offers larger but substantially more variable gains that are most effective when reliable subsymbolic representations are available.

To conclude, NeTheR outperforms its competitors on the revision task in both the structurally informed and uninformed case. Furthermore, the results underscore the effectiveness of NeTheR in combining imperfect knowledge M' with subsymbolic information.

6 Related Work

NeTheR is based on three key features: (1) it leverages an imperfect initial model M' by refining it with (multiple) neural concepts or symbolic literals, (2) it introduces neural concepts that are not pre-defined, (3) thereby combining symbolic and subsymbolic data.

Deep Probabilistic Logic Programming NeSy systems that integrate probabilistic logic programming with neural networks have gained significant attention for their ability to combine reasoning with perception. DeepProbLog (Manhaeve et al. 2021), DeepStochLog (Winters et al. 2022), NeurASP (Yang et al. 2020), and Scallop (Li et al. 2023) are just some examples of systems that enable probabilistic reasoning over the outputs of neural networks. Each of these systems is used under the assumption of perfect symbolic knowledge, where the neural concepts have a predefined intended meaning. In contrast, our contribution does not assume perfect knowledge (key feature 1), and we introduce neural concepts that do not have a pre-envisioned meaning (key feature 2).

Neural predicate invention. Predicate invention systems extend an initial vocabulary with new higher-level predicates that are defined in relation to the existing ones, to improve rule learning. In the neural version, the vocabulary includes neural predicates (Liang et al. 2025; Sha et al. 2024). For example, Sha et al. (2024) explores predicates representing shapes, and other visual features, to learn higher-level concepts in structured visual scenes. Similar to the NeSy systems, these (neural) predicates have a pre-envisioned meaning, and are typically learned before performing predicate invention. In contrast, our work introduces concepts whose meanings are not known a priori (key feature 2) but are instead learned from data alongside the theory, requiring the system to both discover and contextualize their roles without explicit semantic grounding from the user. Recent work on neurosymbolic decision tree learning also introduces neural predicates during structure induction (Möller et al. 2025). In this setting, neural predicates are added as part of a top-down tree construction process and trained jointly with the induced structure. In contrast, our approach uses existing knowledge (key feature 1), allowing neural concepts to be inserted at arbitrary nodes. This enables explicit reasoning about the structural impact of each invented predicate, and allows estimating best- and worst-case performance prior to training the underlying neural network.

Interpretable concept-based models. Concept-based models (CBM) are machine learning models that use human-interpretable concepts as an intermediate layer in its decision-making process. The canonical CBM, named the Concept Bottleneck Model, extracts concepts from raw data using a concept encoder, the results of which are passed to a task predictor that makes the final prediction (Koh et al. 2020). These models have been explored in settings with incomplete or imperfect concepts, aligning with challenges related to imperfect knowledge. Two notable neurosymbolic CBMs that are developed for such settings, DCR (Barbiero et al. 2023) and CMR (Debot et al. 2024), learn logic rules over concepts and utilize neural representations to enhance their accuracy, akin to our notion of neural concepts. Among these, only CMR has the ability to both learn rules and incorporate pre-defined logic rules (key feature 1). This means that, even though CMR was not presented as such, it is a viable solution for our problem setting. However, CMR's use of neural concepts is close to the behavior of *And Or*, while NeTheR allows for a much more refined placement of neural concepts. This explains our empirical observation, that NeTheR is more effective in terms of improving F_1-score while maintaining the integrity of the original input.

Neurosymbolic Structure Learning. The broader idea of revising symbolic knowledge through neural optimization dates back to the neural-symbolic learning cycle proposed in KBANN (Towell and Shavlik 1994) and its successors. These methods translate symbolic theories into neural networks, refine them using gradient-based learning, and in some cases extract refined symbolic theories afterwards (Towell and Shavlik 1993). Our work differs in that it performs theory revision directly within probabilistic logic programming, without translating to and from a separate neural representation. More recent neurosymbolic systems have also explored learning or revising symbolic structure through gradient-based optimization. For example, lifted relational neural networks (Sourek et al. 2015) extend neural-symbolic learning to first-order logic by jointly optimizing neural parameters and relational rule structures, while differentiable ILP approaches such as d-ILP (Shindo et al. 2021) perform end-to-end learning of logical theories using differentiable reasoning. In contrast to these approaches, our work does not aim to learn a symbolic theory from scratch or optimize relational rule sets. Instead, we focus on incrementally revising an existing propositional model through targeted symbolic and neural concept insertions, while preserving tractable probabilistic inference.

Theory revision. Research on theory revision combines human-engineered, rule-based knowledge with empirically learned knowledge using symbolic, probabilistic, and, more recently, neurosymbolic approaches (Ginsberg et al. 1988; Mooney and Shavlik 2021). Classical systems such as DUCE and (N)EITHER (Baffes and Mooney 1993; Muggleton 1987; Ourston and Mooney 1990) refined propositional rule bases using abductive reasoning and inductive learning, while CIGOL, FOCL, FORTE, CLINT, and MIS (Muggleton and Buntine 1988; Richards and Mooney 1991; De Raedt 1992; Kókai et al. 1997) revised first-order Horn clause theories through inductive logic programming. These systems assume that the available symbolic vocabulary is sufficient and therefore revise theories by modifying existing rules or introducing new symbolic predicates. More recent work has expanded the range of theory revision techniques and revision operators. For example, Cerna and Cropper (2024) extend theory revision with predicate invention and negation from a limited number of revision examples, while Morel and Cropper (2023) propose a failure-guided approach to logic program synthesis that similarly uses uncovered failures to guide hypothesis refinement. In probabilistic relational learning, Guimarães et al. (2019) perform online theory revision of ProPPR programs through specialization and generalization operators, while Santos et al. (2020) revise boosted relational dependency networks by editing relational regression trees using local tree-based revision operators. In contrast to these approaches, which revise symbolic or probabilistic theories over predefined symbolic vocabularies, NeTheR extends theory revision to probabilistic-logic-based neurosymbolic models by introducing neural concepts derived directly from subsymbolic data, thereby expanding the symbolic vocabulary beyond concepts that are explicitly available (key feature 3).

Fuzzy Logic Methods. Besides probabilistic logic programming, another major class of neurosymbolic methods combines neural networks with symbolic reasoning through fuzzy semantics. These approaches encode logical formulas as continuous constraints using differentiable t-norms, enabling end-to-end optimization while approximately enforcing logical consistency. Examples include Logic Tensor Networks (Serafini and d'Avila Garcez 2016), Semantic-Based Regularization (Diligenti et al. 2017), and Deep Logic Models (Marra et al. 2019). While these methods differ fundamentally from probabilistic-logic-based probabilistic reasoning, they similarly exploit prior symbolic knowledge to guide neural learning. In contrast, NeTheR focuses on revising the symbolic theory itself within probabilistic logic programming, rather than assuming a fixed logical specification throughout training.

7 Discussion

In this work, we explore the revision of propositional theories by augmenting them with neural concepts. We characterize the trade-off this introduces between interpretability and predictive performance and identify the methodological advances required to generalize the approach to first-order theories.

Interpretability of neural concepts. Neurosymbolic methods combine symbolic reasoning with neural learning, allowing prior knowledge to be incorporated into the model while preserving an explicit symbolic reasoning structure. In NeTheR, this structure is revised locally by introducing symbolic literals and neural concepts. As a result, the overall theory remains inspectable and can be understood in terms of symbolic operations such as conjunction, disjunction, and negation.

Unlike traditional neurosymbolic systems such as DeepProbLog (Manhaeve et al. 2021), however, the neural concepts introduced by NeTheR do not have predefined semantic meanings. Instead, they are latent concepts whose semantics emerge during training. Consequently, NeTheR deliberately trades the semantic interpretability of individual neural concepts for increased expressive power, while retaining an explicit symbolic theory around them. The resulting models therefore remain more auditable than purely neural models. Understanding the semantics of these learned concepts is related to research on interpretability and visualization of neural networks and therefore an important direction for future work. Another promising direction is to improve the interpretability of invented neural concepts through semantic regularization. Since NeTheR already computes the influence set associated with each candidate modification, these examples naturally provide weak supervision on the intended behaviour of the invented concept. Auxiliary objectives based on, for example, contrastive losses, sparsity constraints, concept bottleneck regularization, or disentangled representation learning could encourage the invented neural concepts to represent coherent semantic properties instead of arbitrary latent features. Such regularization could improve the interpretability of invented neural concepts while preserving the flexibility of neural concept invention.

Theoretical guarantees. Since NeTheR performs greedy coordinate ascent over the joint space of symbolic structure and neural parameters, it is not guaranteed to recover the globally optimal revision sequence. Instead, the algorithm performs hill climbing over the space of admissible theory revisions. Since a revision is only accepted when it improves validation performance, the sequence of accepted models is monotonically non-decreasing in validation performance. Furthermore, the stopping criterion terminated the search before reaching the maximum number of iterations in approximately two third of all runs, suggesting that the heuristic is often able to identify a local optimum without exhaustively exploring the entire search space. While this substantially reduces the computational cost of the search in practice, it does not eliminate the possibility that a globally better revision sequence exists.

Future work: generalizing to first-order logic. Extending NeTheR to first-order theories is an important direction for future work. The primary challenge is not the introduction of neural concepts itself, but the substantially larger search space of possible theory revisions. In the propositional setting, the number of candidate insertions is naturally bound by the circuit structure. In contrast, first-order theory revision must additionally determine which predicates, variables, constants, and quantifier structures to introduce, causing the number of admissible revisions to grow combinatorially. Traditional systems such as FORTE (Richards and Mooney 1991) distinguish between revisions that modify existing rules and revisions that introduce new rules through predicate invention. While the former can naturally be extended with neural concepts, the latter presents a considerably larger search problem. Rather than exhaustively enumerating all candidate revisions, a promising direction would be to exploit the extensive literature on inductive logic programming and relational theory revision to constrain the search space using techniques such as language biases, mode declarations, type constraints, or refinement operators (Muggleton and De Raedt 1994; Van Laer and De Raedt 2001). The proposed risk-adjusted ranking heuristic is independent of the underlying symbolic representation and could then be used to prioritize the resulting candidate revisions before expensive neural optimization. Consequently, we view extending NeTheR to first-order logic primarily as a search problem, requiring effective mechanisms for generating a manageable set of candidate revisions while preserving the efficiency of the current framework.

8 Conclusion

We introduced NeTheR, an approach for revising imperfect propositional theories by combining symbolic theory revision with the invention of neurally learned concept representations. To efficiently guide this process, we proposed a risk-adjusted modification selection strategy based on an adapted Sharpe ratio, allowing promising neural revisions to be prioritized before expensive training. Empirical results demonstrate the effectiveness of NeTheR for revising probabilistic-logic-based neurosymbolic models from imperfect initial theories, while also revealing that neural concept insertion is less robust on some non-image datasets where neural networks are trained from scratch. These observations point to opportunities for further improving both the search strategy and the neural optimization process. Overall, NeTheR demonstrates that integrating symbolic theory revision with neural concept invention is a promising direction for revising probabilistic-logic-based neurosymbolic models while preserving an explicit and revisable symbolic structure.

9 Reproducibility

The code for NeTheR and for the experimental evaluation will be released upon paper acceptance. The experimental setup is detailed in Section 5.1, and all evaluations are conducted on open-source datasets, with preprocessing steps described in Appendix D. The proposed algorithm is presented in Section 4.3, and the results of ablation studies are provided in Appendix C.

Acknowledgements

This research received funding from the Flemish Government under the "Onderzoeksprogramma Artificiële Intelligentie (AI) Vlaanderen" programme , from the KU Leuven Research Fund (C14/24/092) and from the European Union (ERC, DeepLog, 101142702). Views and opinions expressed are however those of the author(s) only and do not necessarily reflect those of the European Union or the European Research Council. Neither the European Union nor the granting authority can be held responsible for them. LDR is also supported by the Wallenberg AI, Autonomous Systems and Software Program (WASP) funded by the Knut and Alice Wallenberg Foundation.

References

Ahsan MM, Alam TE, Trafalis TB and Huebner P (2020) Deep MLP-CNN model using mixed-data to distinguish between COVID-19 and non-covid-19 patients. *Symmetry* 12(9): 1526.

Akaike H (1998) *Information Theory and an Extension of the Maximum Likelihood Principle*. New York, NY: Springer New York. ISBN 978-1-4612-1694-0, pp. 199–213. DOI:10.1007/978-1-4612-1694-0_15.

Baffes PT and Mooney RJ (1993) Symbolic revision of theories with m-of-n rules. In: *IJCAI*. Morgan Kaufmann, pp. 1135–1142.

Barbiero P, Ciravegna G, Giannini F, Zarlenga ME, Magister LC, Tonda A, Lio P, Precioso F, Jamnik M and Marra G (2023) Interpretable neural-symbolic concept reasoning. In: *ICML*, *Proceedings of Machine Learning Research*, volume 202. PMLR, pp. 1801–1825.

Benavoli A, Corani G and Mangili F (2016) Should we really use post-hoc tests based on mean-ranks? *J. Mach. Learn. Res.* 17(1): 152–161.

Cassel AB, Mannor S and Zeevi A (2018) A general approach to multi-armed bandits under risk criteria. In: *COLT*, *Proceedings of Machine Learning Research*, volume 75. PMLR, pp. 1295–1306.

Cerna DM and Cropper A (2024) Generalisation through negation and predicate invention. In: *AAAI*. AAAI Press, pp. 10467–10475.

Christ M, Braun N, Neuffer J and Kempa-Liehr AW (2018) Time series feature extraction on basis of scalable hypothesis tests (tsfresh - A python package). *Neurocomputing* 307: 72–77.

Darwiche A and Marquis P (2002) A knowledge compilation map. *J. Artif. Int. Res.* 17(1): 229–264.

De Raedt L (1992) *Interactive Theory Revision: An Inductive Logic Programming Approach*. Academic Press Ltd.

De Raedt L (2008) *Logical and relational learning*. Cognitive Technologies. Springer.

Debot D, Barbiero P, Giannini F, Ciravegna G, Diligenti M and Marra G (2024) Interpretable concept-based memory reasoning. In: *NeurIPS*. pp. 19254–19287.

Defferrard M, Benzi K, Vandergheynst P and Bresson X (2017) FMA: A dataset for music analysis. In: *18th International Society for Music Information Retrieval Conference (ISMIR)*. URL https://arxiv.org/abs/1612.01840.

Demšar J (2006) Statistical comparisons of classifiers over multiple data sets. *J. Mach. Learn. Res.* 7: 1–30.

Diligenti M, Gori M and Saccà C (2017) Semantic-based regularization for learning and inference. *Artif. Intell.* 244: 143–165.

Everingham M, Van Gool L, Williams CKI, Winn J and Zisserman A (2010) The pascal visual object classes (voc) challenge. *International Journal of Computer Vision* 88(2): 303–338.

Fawaz HI, Lucas B, Forestier G, Pelletier C, Schmidt DF, Weber J, Webb GI, Idoumghar L, Muller P and Petitjean F (2020) Inceptiontime: Finding alexnet for time series classification. *Data Min. Knowl. Discov.* 34(6): 1936–1962.

Gartner (2025) Hype cycle for artificial intelligence, 2025. URL https://www.gartner.com/en/newsroom/press-releases/2025-08-05-gartner-hype-cycle-identifies-top-ai-innovations-in-2025. Accessed:2025-02-05.

Gessert N, Nielsen M, Shaikh M, Werner R and Schlaefer A (2020) Skin lesion classification using ensembles of multi-resolution efficientnets with meta data. *MethodsX* 7: 100864. DOI:10.1016/j.mex.2020.100864. URL https://www.sciencedirect.com/science/article/pii/S2215016120300832.

Ginsberg A, Weiss SM and Politakis P (1988) Automatic knowledge base refinement for classification systems. *Artificial Intelligence* 35(2): 197–226. DOI:10.1016/0004-3702(88)90012-4. URL https://www.sciencedirect.com/science/article/pii/0004370288900124.

Guimarães V, Paes A and Zaverucha G (2019) Online probabilistic theory revision from examples with proppr. *Mach. Learn.* 108(7): 1165–1189.

Kawahara J, Daneshvar S, Argenziano G and Hamarneh G (2019) Seven-point checklist and skin lesion classification using multitask multimodal neural nets. *IEEE Journal of Biomedical and*

Health Informatics 23(2): 538–546. DOI:10.1109/JBHI.2018.2824327.

Khurshid S, Abdulla MS and Ghatak G (2025) Optimizing sharpe ratio: risk-adjusted decision-making in multi-armed bandits. *Mach. Learn.* 114(2). DOI:10.1007/s10994-024-06680-2.

Koh PW, Nguyen T, Tang YS, Mussmann S, Pierson E, Kim B and Liang P (2020) Concept bottleneck models. In: *ICML*, *Proceedings of Machine Learning Research*, volume 119. PMLR, pp. 5338–5348.

Kókai G, Harmath L and Gyimóthy T (1997) Algorithmic debugging and testing of prolog programs. In: *LPE*. pp. 14–21.

Li Z, Huang J and Naik M (2023) Scallop: A language for neurosymbolic programming. *Proc. ACM Program. Lang.* 7(PLDI): 1463–1487.

Liang Y, Kumar N, Tang H, Weller A, Tenenbaum JB, Silver T, Henriques JF and Ellis K (2025) Visualpredicator: Learning abstract world models with neuro-symbolic predicates for robot planning. In: *ICLR*. OpenReview.net, pp. 60416–60444.

Liu Z, Luo P, Wang X and Tang X (2015) Deep learning face attributes in the wild. In: *Proceedings of International Conference on Computer Vision (ICCV)*. pp. 3730–3738.

Mahoney JJ and Mooney RJ (1993) Combining connectionist and symbolic learning to refine certainty factor rule bases. *Connection Science* 5(3-4): 339–364. DOI:10.1080/09540099308915704.

Manhaeve R, Dumancic S, Kimmig A, Demeester T and De Raedt L (2021) Neural probabilistic logic programming in deepproblog. *Artif. Intell.* 298: 103504.

Marra G, Giannini F, Diligenti M and Gori M (2019) Integrating learning and reasoning with deep logic models. In: *ECML/PKDD (2)*, *Lecture Notes in Computer Science*, volume 11907. Springer, pp. 517–532.

Meert W (2017) Pysdd. *Recent Trends in Knowledge Compilation (Dagstuhl Seminar 17381),Dagstuhl Reports* 7(9): 81.

Mooney RJ and Shavlik JW (2021) A recap of early work on theory and knowledge refinement. In: *AAAI Spring Symposium: Combining Machine Learning with Knowledge Engineering*, *CEUR Workshop Proceedings*, volume 2846. CEUR-WS.org, pp. 1–9.

Morel R and Cropper A (2023) Learning logic programs by explaining their failures. *Mach. Learn.* 112(10): 3917–3943.

Muggleton SH (1987) Duce, an oracle-based approach to constructive induction. In: *IJCAI*. Morgan Kaufmann, pp. 287–292.

Muggleton SH and Buntine WL (1988) Machine invention of first order predicates by inverting resolution. In: *ML*. Morgan Kaufmann, pp. 339–352.

Muggleton SH and De Raedt L (1994) Inductive logic programming: Theory and methods. *J. Log. Program.* 19/20: 629–679.

Möller M, Norlander A, Martires PZD and De Raedt L (2025) Neurosymbolic decision trees. URL https://arxiv.org/abs/2503.08762.

Ourston D and Mooney RJ (1990) Changing the rules: A comprehensive approach to theory refinement. In: *AAAI*. AAAI Press / The MIT Press, pp. 815–820.

Pav SE (2021) *The Sharpe Ratio: Statistics and Applications*. Chapman and Hall/CRC.

Pierce E (2021) Austin Housing Prices. https://www.kaggle.com/datasets/ericpierce/austinhousingprices. [Accessed 15-11-2024].

Ramachandran S and Mooney RJ (1996) Revising bayesian network parameters using backpropagation. In: *Proceedings of the International Conference on Neural Networks (ICNN-96), Special Session on Knowledge-Based Artificial Neural Networks*. Washington DC, pp. 82–87. URL http://www.cs.utexas.edu/users/ai-lab?ramachandran:icnn96kbai.

Rebbapragada U, Protopapas P, Brodley CE and Alcock CR (2009) Finding anomalous periodic time series: An application to catalogs of periodic variable stars. *CoRR* abs/0905.3428.

Richards BL and Mooney RJ (1991) First-order theory revision. In: *ML*. Morgan Kaufmann, pp. 447–451.

Rudin C, Chen C, Chen Z, Huang H, Semenova L and Zhong C (2021) Interpretable machine learning: Fundamental principles and 10 grand challenges. *CoRR* abs/2103.11251.

Russell S and Norvig P (2020) *Artificial Intelligence: A Modern Approach (4th Edition)*. Pearson.

Santos RA, Paes A and Zaverucha G (2020) Transfer learning by mapping and revising boosted relational dependency networks. *Mach. Learn.* 109(7): 1435–1463.

Schwarz G (1978) Estimating the Dimension of a Model. *The Annals of Statistics* 6(2): 461 – 464. DOI:10.1214/aos/1176344136.

Serafini L and d'Avila Garcez AS (2016) Learning and reasoning with logic tensor networks. In: *AI*IA*, *Lecture Notes in Computer Science*, volume 10037. Springer, pp. 334–348.

Sha J, Shindo H, Delfosse Q, Kersting K and Dhami DS (2024) EXPIL: explanatory predicate invention for learning in games. *CoRR* abs/2406.06107.

Shindo H, Nishino M and Yamamoto A (2021) Differentiable inductive logic programming for structured examples. In: *AAAI*. AAAI Press, pp. 5034–5041.

Song Y, Demirdjian D and Davis R (2011) Tracking body and hands for gesture recognition: NATOPS aircraft handling signals database. In: *FG*. IEEE Computer Society, pp. 500–506.

Sortino FA and Price LN (1994) Performance measurement in a downside risk framework. *The Journal of Investing* 3. DOI:10.3905/joi.3.3.59.

Sourek G, Aschenbrenner V, Zelezný F and Kuzelka O (2015) Lifted relational neural networks. In: *CoCo@NIPS*, *CEUR Workshop Proceedings*, volume 1583. CEUR-WS.org.

Towell GG and Shavlik JW (1993) Extracting refined rules from knowledge-based neural networks. *Mach. Learn.* 13: 71–101.

Towell GG and Shavlik JW (1994) Knowledge-based artificial neural networks. *Artif. Intell.* 70(1-2): 119–165.

Van Laer W and De Raedt L (2001) How to upgrade propositional learners to first order logic: A case study. In: *Machine Learning and Its Applications*, *Lecture Notes in Computer Science*, volume 2049. Springer, pp. 102–126.

Van Wesenbeeck D, Yurtman A, Meert W and Blockeel H (2024) Quantitative evaluation of motif sets in time series. URL https://arxiv.org/abs/2412.09346.

Wah C, Branson S, Welinder P, Perona P and Belongie S (2011) The caltech-ucsd birds-200-2011 dataset. Technical Report CNS-TR-2011-001, California Institute of Technology.

Winters T, Marra G, Manhaeve R and De Raedt L (2022) Deepstochlog: Neural stochastic logic programming. In: *AAAI*. AAAI Press, pp. 10090–10100.

Wright SJ (2015) Coordinate descent algorithms. *Math. Program.* 151(1): 3–34.

Xi G, Tao C and Zhou Y (2021) Near-optimal MNL bandits under risk criteria. In: *AAAI*. AAAI Press, pp. 10397–10404.

Xian Y, Lampert CH, Schiele B and Akata Z (2019) Zero-shot learning - A comprehensive evaluation of the good, the bad and the ugly. *IEEE Trans. Pattern Anal. Mach. Intell.* 41(9): 2251–2265.

Yang Z, Ishay A and Lee J (2020) Neurasp: Embracing neural networks into answer set programming. In: *IJCAI*. ijcai.org, pp. 1755–1762.

A Number of possible modifications

Given a circuit with l literals, n neural concepts and i inner nodes, we consider the following modifications:

- A removal modification can apply to every leaf node, thus giving $l+n$ possibilities.
- A new symbolic literal can be added to each leaf node, to the root node and as a child node to each inner node, thus resulting in $(l+n+i+1)$ possibilities
- A new neural concept can be added to each leaf node, to the root node and as a child node to each inner node that does not already have a neural concept as a child, thus resulting in $(l+i-n+1)$ possibilities

This sums up to $3*l+2*i+n+2$. In the edge cases that the circuit consists of a single neural concept or a single literal, the formula is $2*l+2*i+2$ as removal operations are not allowed in this case.

B Modification Selection Example

To clarify how the Sharpe ratio is used to select the next modification, consider the following toy example. This is based on the circuit used in Figure 1.

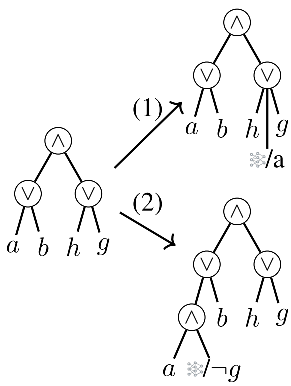

ID	a	b	h	g	Label
1	✓	✓	✓	✓	✓
2	✓	✗	✓	✗	✓
3	✗	✓	✗	✓	✓
4	✓	✓	✗	✗	✓
5	✓	✗	✗	✗	✓
6	✗	✓	✗	✗	✓
7	✓	✗	✗	✓	✗
8	✓	✗	✓	✗	✗
9	✗	✓	✗	✗	✗
10	✗	✗	✗	✗	✗

The initial circuit covers instances $\{1,2,3,7,8\}$, thus yielding:

$$TP=\{1,2,3\},\quad FP=\{7,8\},\quad FN=\{4,5,6\},\quad TN=\{9,10\}.$$

This leads to an initial performance:

$$F_1=\frac{2|TP|}{2|TP|+|FP|+|FN|}=\frac{6}{11}\approx 0.55.$$

We consider two candidate neural modifications:

1. inserting a neural concept in disjunction with the existing subcircuit $(h\vee g)$,
2. inserting a neural concept in conjunction with literal a.

Influence sets. The influence sets determine exactly which examples can be affected by each modification.

Modification 1 (generalisation). This replaces a node n with $n' = n \vee m$. The generalisation influence set is:

$$E_{\text{gen}}^{(1)} = \{4, 5, 6, 9\}.$$

These are precisely the examples currently classified as negative that would become positive if node n evaluated to true:

$$M[n \leftarrow True](x) = 1.$$

Examples outside this set, such as instance 10, remain unaffected.

Modification 2 (specialisation). This replaces a node n with $n' = n \wedge m$. The specialisation influence set is:

$$E_{\text{spec}}^{(2)} = \{2, 7, 8\}.$$

These are precisely the examples currently classified as positive that would become negative if node n evaluated to false:

$$M[n \leftarrow False](x) = 0.$$

Examples outside this set remain unaffected.

Best and worst case performance. The best and worst cases correspond to probability functions acting optimally or adversarially on the corresponding influence set, while leaving all other predictions unchanged.

Modification 1 (generalisation).

Only examples in $E_{\text{gen}}^{(1)}$ can change.

Best case.

The optimal probability function satisfies: $p^*(x) = \begin{cases} 1 & x \in \{4, 5, 6\} \\ 0 & x = 9 \end{cases}$

This yields: $TP = \{1, 2, 3, 4, 5, 6\}, \quad FP = \{7, 8\}, \quad FN = \emptyset.$

Thus, $B_1 = \frac{12}{12+2+0} = \frac{12}{14} \approx 0.86.$

Worst case.

The adversarial probability function satisfies:$p_\perp(x) = \begin{cases} 1 & x = 9 \\ 0 & x \in \{4, 5, 6\} \end{cases}$

This yields: $TP = \{1, 2, 3\}, \quad FP = \{7, 8, 9\}, \quad FN = \{4, 5, 6\}.$

Thus, $W_1 = \frac{6}{6+3+3} = \frac{6}{12} = 0.5.$

Modification 2 (specialisation).

Only examples in $E_{\text{spec}}^{(2)}$ can change.

Best case.

The optimal probability function satisfies: $p^*(x) = \begin{cases} 0 & x \in \{7, 8\} \\ 1 & x = 2 \end{cases}$

This yields: $TP = \{1, 2, 3\}, \quad FP = \emptyset, \quad FN = \{4, 5, 6\}$.

Thus, $B_2 = \frac{6}{6+0+3} = \frac{6}{9} \approx 0.66$.

Worst case.

The adversarial probability function satisfies: $p_\perp(x) = \begin{cases} 0 & x = 2 \\ 1 & x \in \{7, 8\} \end{cases}$

This yields: $TP = \{1, 3\}, \quad FP = \{7, 8\}, \quad FN = \{2, 4, 5, 6\}$.

Thus, $W_2 = \frac{4}{4+2+4} = \frac{4}{10} = 0.4$.

Risk-free modification. To calculate the risk-free rate for the Sharpe ratio, we measure the performance of all symbolic operations. In this example, we consider all removal operations and two operations adding a symbolic literal in the same places as the neural concepts, with the decision stump learned on the influence sets from above:

Removing a from the circuit results in $\mathrm{F}_1 = \frac{4}{4+0+4} = \frac{4}{8} = 0.5$
Removing b from the circuit results in $\mathrm{F}_1 = \frac{4}{4+2+4} = \frac{4}{10} = 0.4$
Removing h from the circuit results in $\mathrm{F}_1 = \frac{4}{4+1+4} = \frac{4}{9} \approx 0.44$
Removing g from the circuit results in $\mathrm{F}_1 = \frac{4}{4+1+4} = \frac{4}{9} \approx 0.44$
Adding a literal (a) in disjunction with $h \vee g$ results in $\mathrm{F}_1 = \frac{10}{10+2+1} = \frac{10}{13} \approx 0.77$
Adding a literal $(\neg g)$ in conjunction with a results in $\mathrm{F}_1 = \frac{6}{6+1+3} = \frac{6}{10} = 0.6$
Performing no modification: $\mathrm{F}_1 = 0.55$

The best risk-free modification $R_f = 0.77$ is thus adding a symbolic concept in disjunction as in modification 1.

Calculating the Sharpe ratio. Say that we do not have prior information over the performance of the neural network, thus setting $\alpha = 0.5$. The Sharpe ratios of both modifications are then calculated as shown in equation (4):

$$S_1 = \frac{\alpha B_1 + (1-\alpha) W_1 - R_f}{\sqrt{\alpha((1-\alpha)B_1 - (1-\alpha)W_1)^2 + (1-\alpha)(\alpha W_1 - \alpha B_1)^2}} = -0.44$$

In similar fashion, we calculate $S_2 = -1.77$, thus showing that applying the risk-free symbolic modification would result in the best estimated performance gain. In the case that there is prior information that the neural network performs better than average, $\alpha = 0.8$, the Sharpe ratios change. The first neural modification would then have $S_1 = 0.19$, the second would have $S_2 = -1.46$, thus showing that in this case applying the first neural modification has a higher estimated gain than performing the risk-free symbolic modification in the same place.

C Ablation Studies

The ablation studies were conducted using the experimental setup with structural information.

C.1 Effectiveness of the Selection Heuristic

This experiment evaluates the proposed selection heuristic along two dimensions. First, we compare the proposed dynamic update of α against the static alternatives described in Section 4.2. Second, we compare the Sharpe-ratio-based heuristic with the Sortino ratio, which penalizes only downside risk and was suggested as an alternative risk-adjusted selection criterion.

The results, shown in Figure 5 and Table 6, demonstrate that the proposed dynamic Sharpe ratio outperforms all alternative approaches. Dynamically updating α enables the heuristic to adapt its estimate of the expected reward and uncertainty of neural insertions throughout the revision process, resulting in more reliable revision decisions than static estimates.

Furthermore, replacing the Sharpe ratio with the Sortino ratio degrades performance. While the Sortino ratio discounts upside variance and therefore encourages more optimistic neural insertions, this leads to an overestimation of neural concepts whose performance is difficult to predict. This effect is particularly pronounced on the non-image datasets, where neural concepts must be learned from scratch rather than fine-tuned from pretrained feature extractors. In these settings, the more conservative uncertainty estimate provided by the Sharpe ratio yields substantially better revision decisions, demonstrating that penalizing symmetric uncertainty is beneficial for neural theory revision.

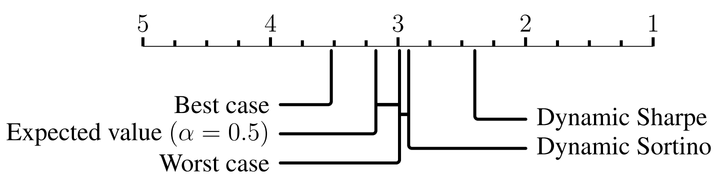

Figure 5. Critical difference diagram, identifying the dynamic Sharpe ratio as the best heuristic. Closer to 1 is better.

C.2 Freezing Existing Neural Concepts

When adding a neural concept, the underlying neural network is trained using indirect supervision while freezing the parameters of the previously trained neural networks. Table 7 shows the results of running NeTheR with only neural modifications allowed, in the cases that the result was modified with at least two neural concepts. It is clear that this choice, of freezing previously learned parameters does not significantly affect classification performance. In contrast to runtime, where it enhances computational

Table 6. F_1-score results of ablation study 1, which studies the used selection heuristic. The dynamic Sharpe ratio outperforms the static approaches.

Datasets	Sharpe dynamic	Sortino dynamic	Worst case	Sharpe $\alpha = 0.5$	Best case
ATH	0.87 ± 0.11	0.87 ± 0.11	0.87 ± 0.11	0.87 ± 0.11	0.86 ± 0.11
AWA2	0.87 ± 0.09	0.87 ± 0.09	0.84 ± 0.10	0.84 ± 0.10	0.86 ± 0.09
CelebA	0.89 ± 0.11	0.90 ± 0.10	0.87 ± 0.11	0.88 ± 0.11	0.88 ± 0.10
CUBB	0.89 ± 0.09	0.89 ± 0.09	0.87 ± 0.10	0.88 ± 0.10	0.89 ± 0.10
derm7pt	0.84 ± 0.12	0.83 ± 0.12	0.82 ± 0.14	0.83 ± 0.14	0.82 ± 0.12
FMA	0.83 ± 0.11	0.64 ± 0.23	0.82 ± 0.11	0.63 ± 0.25	0.51 ± 0.19
motifs	0.83 ± 0.13	0.64 ± 0.27	0.79 ± 0.14	0.76 ± 0.17	0.57 ± 0.23
Pascal VOC	0.89 ± 0.10	0.89 ± 0.09	0.85 ± 0.11	0.87 ± 0.11	0.88 ± 0.09
StarLightCurves	0.84 ± 0.11	0.80 ± 0.15	0.84 ± 0.11	0.82 ± 0.13	0.61 ± 0.27

efficiency, as the number of trainable parameters is reduced in subsequent iterations, thereby decreasing the computational load and memory requirements for optimization.

Table 7. Results of ablation study 2, which studies the effect of freezing existing learned neural concepts. The results show that there are minor differences in F_1-score, but major differences in runtime.

Datasets	**Freeze**		**No Freeze**	
	F_1	time (s)	F_1	time (s)
ATH	0.86 ± 0.12	2579	0.87 ± 0.13	3080
AWA2	0.87 ± 0.10	784	0.86 ± 0.10	850
CelebA	0.95 ± 0.03	1084	0.95 ± 0.03	1351
CUBB	0.90 ± 0.10	2150	0.90 ± 0.10	2331
derm7pt	0.86 ± 0.13	303	0.87 ± 0.11	322
FMA	0.81 ± 0.17	718	0.78 ± 0.21	863
motifs	0.66 ± 0.28	883	0.62 ± 0.30	1196
Pascal VOC	0.89 ± 0.08	3637	0.89 ± 0.08	3913
StarLightCurves	0.86 ± 0.18	2727	0.85 ± 0.19	4468

C.3 Data-efficiency

We evaluate the data-efficiency by varying the size of the training dataset, for all datasets. Based on the previous performance results, we excluded *And Or* and *Or And* from the comparison because they are worse versions of NeTheR. The results of the data-efficiency experiment are shown in Figure 6 and Table 8. Both NeTheR and *CMR* perform much better in low data regimes because they can rely on M'. Compared to *CMR*, NeTheR shows slightly better but similar performance.

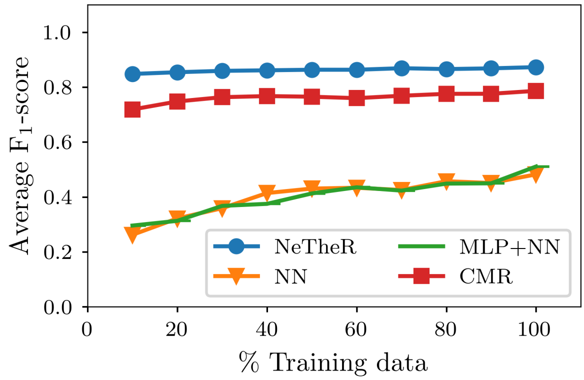

Figure 6. NeTheR is robust to limited training data.

Table 8. Numerical results showing the average F_1-score over all datasets per fraction (%) of available training data. It is clear that both NeTheR and CMR are robust against limited training data.

Methods	F_1-score per fraction of available data									
	10%	20%	30%	40%	50%	60%	70%	80%	90%	100%
NeTheR	0.85	0.85	0.86	0.86	0.86	0.86	0.87	0.87	0.87	0.88
CMR	0.72	0.75	0.76	0.77	0.77	0.77	0.77	0.78	0.78	0.79
NN	0.26	0.32	0.36	0.41	0.43	0.43	0.43	0.46	0.46	0.48
MLP+NN	0.30	0.31	0.37	0.37	0.41	0.44	0.44	0.45	0.45	0.51

D Experiment details

We consider multiple benchmark datasets, the details of which we list below. We also clarify the generation of ground truth theories M^* and imperfect theories M'.

D.1 Benchmark Datasets

Austin Texas Housing (ATH) (Pierce 2021). All images were resized to 64×64 pixels, and irrelevant attributes (zpid, description, streetAddress, zipcode, latitude, longitude, latest_saledate) were removed to streamline the dataset for the task.

AWA2 (Xian et al. 2019). All images were resized to 64×64 pixels and used as subsymbolic data. The provided predicates associated with each class were utilized as symbolic data.

CelebA (Liu et al. 2015). We used the first 10,000 images in this dataset, all resized to 64x64 pixels. The attributes related to each picture were used as symbolic data.

CUB (*Wah et al. 2011*). All images were resized to 64×64 pixels and used as subsymbolic data. The provided attributes associated with each picture that had $certainty \in \{guessing, probably, definitely\}$ were utilized as symbolic data.

derm7pt (*Kawahara et al. 2019*). The clinical images were resized to 64x64 pixels and used as subsymbolic data. The given metadata and 7-point structure attributes were used as symbolic data.

FMA (*Defferrard et al. 2017*). For this dataset, we used the 'large' subset and discretized both the track data and Echonest data to obtain symbolic representations. The provided audio features were retained as subsymbolic data for analysis.

Motifs. This dataset comprises time series that were generated using TSMD-Bench (Van Wesenbeeck et al. 2024), constructed from the six core motifs from the NATOPS time series (Song et al. 2011). We extended these six core motifs to 18, by shifting their amplitude with +2 or -2. This simulates a common occurrence, for example, leakages cause a fixed amplitude to existing patterns. This is a challenging component in time series classification tasks, as instances have to be differentiated in both amplitude and shape. Then, using these 18 motifs, we generated 10,000 random instances by concatenating 10 random motifs per instance. Each instance thus comprises 180 Boolean values as symbolic data, indicating whether a specific motif appears in a particular position. Figure 7 illustrates half of an instance with its symbolic representation.

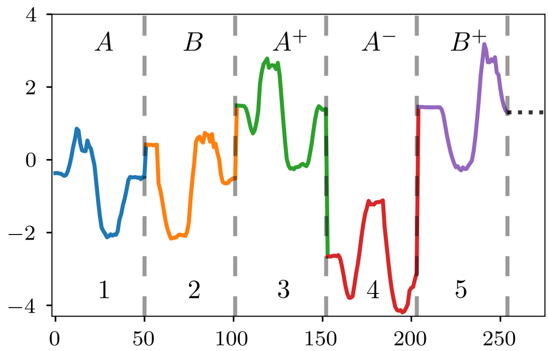

Figure 7. Visualization of five windows of one instance in the motifs dataset. X_i^+ and X_i^- both denote motif X in window i, with respectively a positive and negative shift in amplitude. The symbolic data of this instance would be $\{A_1{=}\top, B_2{=}\top, A_3^+{=}\top, A_4^-{=}\top, B_5^+{=}\top\}$, with the remaining variables $\bot$.

Pascal VOC (*Everingham et al. 2010*) All images were resized to 64×64 pixels and used as subsymbolic data. We used the presence of an object in the image as symbolic data.

StarLightCurves (Rebbapragada et al. 2009). Each instance in this time series dataset was divided into three equal windows. Within each window, the following features were identified: large peak, deep trough, low variability, high variability, sinusoidal shape, high average and large difference between min and max. Such features can be computed automatically and are often used in deployed systems (Christ et al. 2018). Each feature-window combination was represented as a Boolean variable to mimic expert detection of anomalies or behaviours based on patterns in specific parts of the time series.

D.2 Generating M* and M'.

For each dataset, we generated 24 logic circuits M^* and corresponding imperfect circuits M'. The construction process for M^* is top-down, starting from a disjunctive root node and iteratively refining the lower nodes. Each branch of the root disjunction contains nested conjunction nodes, and the leaf nodes are atomic variable comparisons using categorical or continuous columns from the data (e.g., $age < 30$ or $temperature = High$). Each node is generated with a degree of randomness, becoming either a nested subtree or a leaf node. In case of the latter, a random valid option (attribute, comparison operator and value) is chosen based on the dataset. The structurally informed imperfect theory M' is obtained from M^* by selecting a set of random attributes that are present within M^*, and by removing all leaf nodes using those variables. If the resulting M' has an F_1-score that is not between 0.6 and 0.9, the process for generating an M^* and corresponding M' starts over. This resulted in M^* circuits that range from 3 to 47 nodes with a mean and standard deviation of 14 ± 9 nodes, with corresponding M' circuits ranging from 1 to 39 nodes and a mean and standard deviation of 8 ± 8 nodes. To learn the decision trees for the experiment without structural information, we use the training data and alter the parameters of the sklearn decision tree learner until the tree has an F_1-score smaller than 0.9.

E Experiment On Existing Labels

The experiments in Section 5 are conducted on the generated target model M^*. In this section we again repeat the non-informed experiment, but now using the existing labels of the dataset. We focus on derm7pt as it is a binary classification task, inferring the presence of melanoma. Instead of using the multitask approach that is proposed in the original paper (Kawahara et al. 2019), we learned a classifier (ResNet-50) for each of the 7-point structures using both the dermoscopic and clinical images.

After that, we use the predicted values for the 7-point structures to construct the 7-pt score, which is combined with the metadata to serve as the data to learn a decision tree on. This decision tree can then be revised using NeTheR with both the dermoscopic and clinical images as subsymbolic data. We include as reference the models that were specifically designed for this task, and that were trained on unbalanced datasets: the 7pt-Unbalanced and Direct-unbalanced results that can be found in the benchmark paper (Kawahara et al. 2019). Table 9 summarizes the results, showing that the learned decision tree already outperforms the originally proposed approaches, and that NeTheR further improves performance.

Table 9. AUROC scores on the melanoma inferring task of the derm7pt dataset.

Methods	AUROC-score
Kawahara et al. (7pt-Unbalanced)	76.8
Kawahara et al. (Direct-Unbalanced)	83.2
Learned Decision Tree (M')	85.0
NeTheR	86.9

F Hardware

The experiments are performed on a machine running Ubuntu 20.04.6 LTS with 128 GB memory, an Intel(R) Xeon(R) CPU E5-2630 v4 @ 2.20GHz CPU and a NVIDIA GeForce GTX 1080 Ti GPU.

G Qualitative examples

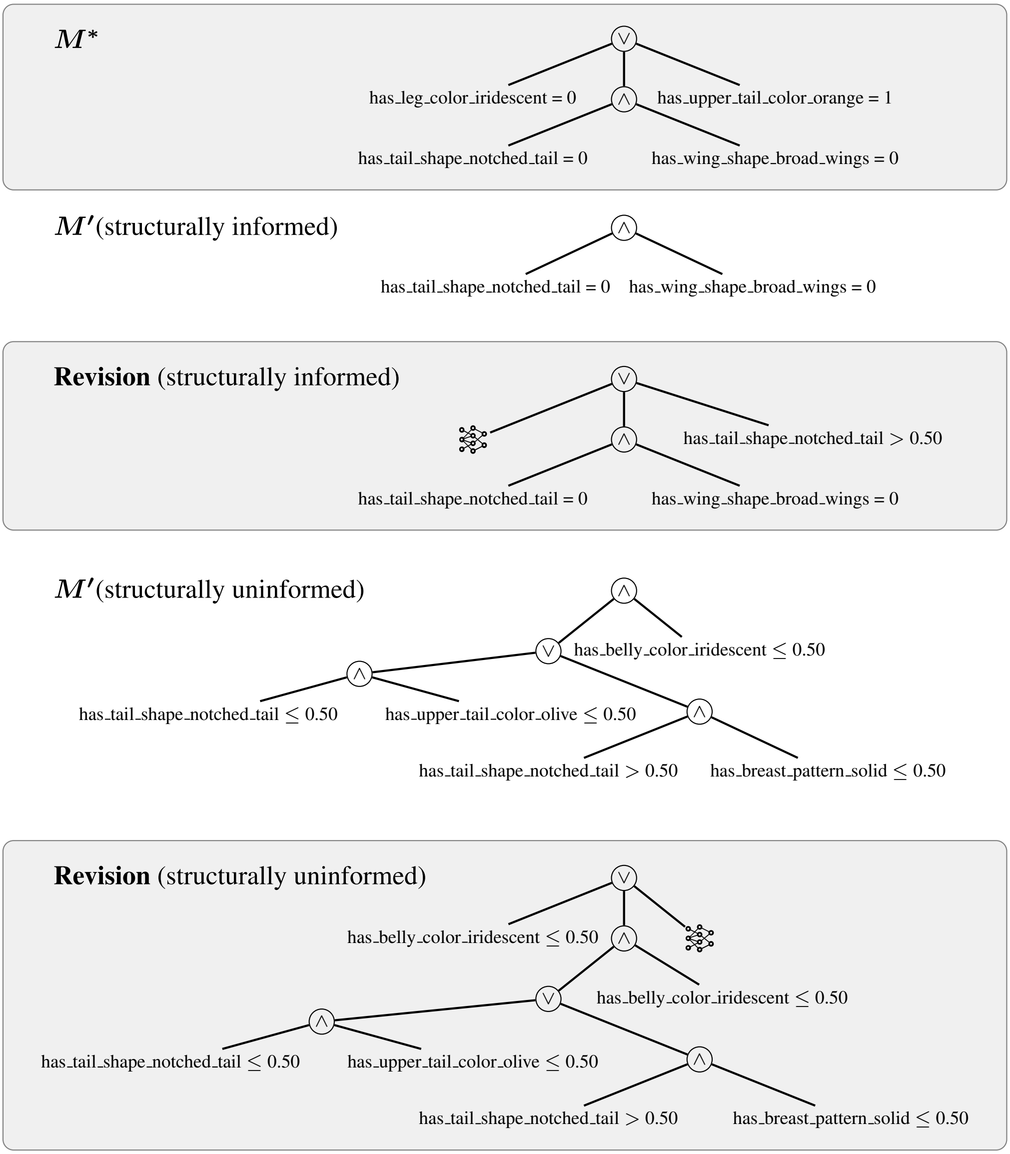

Figure 8. An example of an instance of the CUB dataset. The F_1-score for the structurally informed experiment increased from 0.78 for M' to 0.99 for the revised model of NeTheR that introduced a neural concept and a new symbolic literal. For the uninformed experiment, the learned decision tree reached an F_1-score of 0.89, while its revision using NeTheR outperforms with an F_1-score of 0.99.